가압유동층연소로의 수학적 모델

December 7th, 2000

군산대학교 화학공학과 송병호

1. 서론

가압유동층 연소로 – Pressure effects

- 가압에 따른 가스 밀도의 증가가 유동화 거동에 가장 큰 영향을 미친다.
- 최소유동화속도가 감소하여서 가스의 층내 체류시간이 증대된다.

- 더 작은 기포들이 더 많이 생긴다 (특히 A 군 입자에서)
- Bubble diameter should decrease with pressure (King, 1979).
- 압력의 증가에 따라 공극율은 1 – 4% 정도 증가.

- Geldart B 군 입자에서는 에멀젼상의 공극율(void fraction),
  기포의 형상 및 크기가 별로 변하지 않는다.

- 기포흐름양이 증가하고, 종말속도 감소하므로 입자비산은 증가함.

- Dense phase 로부터 char로의 산소 확산을 살펴보면,

$$Sh = a + b\,\mathrm{Re}^{1/2}\,Sc^{1/3}$$

Sh is only slightly sensitive to pressure, increasing with $P^{0.75}$ at maximum.
산소의 분자확산계수는 압력의 1승에 반비례한다:
결국, 물질확산계수는 압력의 증가에 따라 약간 감소한다.

$$k_{diff} = \frac{Sh \cdot D_G}{2r_i}$$

그러나 산소의 부분압이 증가하여 총괄 연소속도는 결국 증가한다.

Table 1-1. Models for predicting carbon efficiency in continuous FBC

(a) Models

reference	A	B	C	D	E	F	G	H
Campbell and Davidson, 1975	I	a	I	c	I	c	no	no
Gibbs, 1975	I	a	I	a	I	a,b	no	no
Gordon and Amundson, 1976	I	a	I	c	I-III	c	no	yes
Baron et al., 1977	I-IV	a-d	I	b	II	a,b	no	no
Chen and Saxena, 1977	II	c	I	c	I	a	no	no
Baron et al., 1978	I	a	I	c	I	a	no	no
Chen and Saxena, 1978	II	a	II	c	I	a	no	no
Gordon et al., 1978	I	a	I	c	III	c	no	yes
Horio and Wen, 1978	III	b	II	a	II	a	no	yes
Rajan et al., 1978	III	b	II	a	II	a	no	yes
Donsi et al., 1979	I	a,b	I	b	II	a,b	yes	yes
Fan et al., 1979	I	a	III	c	I	c	no	no
Park et al., 1981	IV	d	I	d	II	a	yes	yes
Bywater, 1980	IV	d	III	f	II	c	no	no
Rajan and Wen, 1980	III	b	II	c	II	a,b	yes	yes
Bukur and Amundson, 1981	I	a	I	c	I	a	no	yes
Congalidis and Georgakis, 1981	III	a	II	b	III	a,b	no	yes
Tojo et al., 1981	I	a	III	c	I	c	no	no
Tung et al., 1981	I	a	I	b	II	a	no	no
Overturf and Reklaitis, 1983	I-IV	a-d	I	b	III	a,b	no	yes
Miccio and Salatino, 1985	I	a	I	a	II	b	no	no
Lemcoff, 1988	I	a-c	I	c	III, IV	c	no	yes
Chandran and Sutherland, 1988	IV	d	III	e,f	II	a,b	yes	yes
Ho et al., 1989	I-IV	b	III	b	III	a	no	no
Azevedo et al., 1989	III	b,c	II	a,b	III	a,b	no	yes
Souza-Santos, 1989	I	a	I	d	III	a	yes	yes
Westby et al., 1990	I	a	I	a	I	a	no	no

(b) Description of the models

A. model for fluidized bed
  I. two-phase bubbling bed model: bubble and emulsion phase
  II. three-phase bubbling bed model: bubble, cloud, and emulsion phase
  III. compartments in series model: two phases in each compartment
  IV. slow bubble regime model: no distiction made between the bubble phase and the emulsion phase

B. gas flow pattern in the bed
  a. plug flow in the bubble phase, mixed flow in the emulsion phase
  b. mixed flow in both phases
  c. plug flow in both phases; gas exchange between two phases is finite
  d. plug flow through the bed; no distiction between phases

C. movement of solids in the bed
  I. well mixed
  II. well mixed in a number of compartments
  III. dispersion of solids is finite; dispersion coefficient is used for mass balance

D. devolatilization of feed coal
  a. instantaneous devolatilization; volatiles evolve uniformly across the plane of coal feed point
  b. devolatilization is slower than mixing of the feed coal; volatiles evolve uniformly throughout the bed
  c. not considered
  d. devolatilization is instantaneous at the feed point
  e. devolatilization is apportioned between (b) and (d)
  f. devolatilization occurs as solids diffuse; volatiles undergo diffusion-controlled combustion

E. kinetics of solid coal combustion
  I. film diffusion controlling
  II. both film diffusion and surface reaction influence the rate, but homogeneous oxidation of CO to CO2 is assumed to be very fast
  III. rate of CO oxidation is comparable to that of other reactions
  IV. includes ash layer of diffusion

F. elutriation considered?
  a. char burns to elutriable size
  b. attrition allowed for
  c. not considered

G. freeboard combustion considered?

H. heat balance around char particle?

Table 1-2. Summary of characteristics of previous models.

저 자	모 델 설 명
Sengupta and Basu (1991)	- Cell model - 축방향으로 고체의 net flux를 외부순환속도로 고려. 그러나 이 가정이 모델의 오차에 기여. - 촤입자의 연소속도를 탄소의 반응속도와 마모속도의 합으로 고려한다. - 촤의 입자수지만 고려하고, 층물질의 입자수지는 제외됨. - 하부의 조밀상에서 촤의 입자수지에서 분쇄 및 마모의 영향이 무시됨. - 2차공기의 영향을 고려한다.
Zhang *et al.* (1991)	- Dynamic model, cell model - 축방향 고체체유량, 입자비산속도에 관한 상관식 사용 - 입도별 마모속도는 고려하고 있으나, 동일입도에서 탄소농도분포에 대해서는 고려 않음. - 모델설명이 불분명하다.
Lin and Li (1993)	- Cell model - 축방향 고체체유량분포를 주어진 조건으로 사용함. - 층물질의 입자수지는 제외됨.
Xiangdong and Jianxiong (1993)	- Cell model - 입도별 입자수지는 고려된 것 같으나 탄소농도별 입자수지는 불분명. 전체적인 모델구조에 대한 설명 불분명.
Adanez *et al.* (1995)	- 단일계 해석 - 축방향 고체체유량, 조밀상표면에서 고체비산속도, 희박상에서 고체의 분산계수를 고려. - 촤와 회분의 수지를 별도로 고려하고, 입도만을 변수로 함. - 연소하는 촤입자로부터 회분입자가 생성되는 별도의 모델을 사용.

Hannes *et al.* (1995) – IEA model
– Dense phase 에 기포유동층 모델을 사용함.
– 촤와 회분의 수지를 별도로 고려하고, 입도만을 변수로 함.
– 석탄과 석회석 마모도 고려하였음.

Heinbockel and Fett (1995) – 가압 CFBC 연소로 모델, Cell model
– 촤와 회분의 수지를 별도로 고려하고, 입도만을 변수로 함.

Legros *et al.* (1995) – ASPEN PLUS에 의한 모델, Cell model
– 고체체유량분포, 고체유량, 촤의 연소에 관한 정보가 중요함.
– 층물질의 입자수지는 제외.

Choi (1989) – 1차원 모델, 상압 기포층
– 유동특성, 입도만을 고려한 입자수지, 외부 입자순환속도(입자비산속도)가 고려되었음. 고회분 석탄에 적용됨

Choi et al. (1996, 1997) – CFBC 모델
– 다단공기주입, 입도와 탄소농도를 동시에 고려한 입자수지, 석탄의 연소, 탈황특성, 축방향 입자농도분포, 외부 입자순환속도 등을 고려.

Song et al.(1996) – PFBC 에서 석탄 연소효율에 대한 압력의 영향을 예측하는 간단한 모델.

1. Combustion of coal

- Time scale of Solids mixing, 3 – 10 sec
- Release and combustion of volatile matter, 5 – 20 sec
- Combustion of the remaining char, 100 – 500 s.
- Heat transfer, 100 – 200 sec

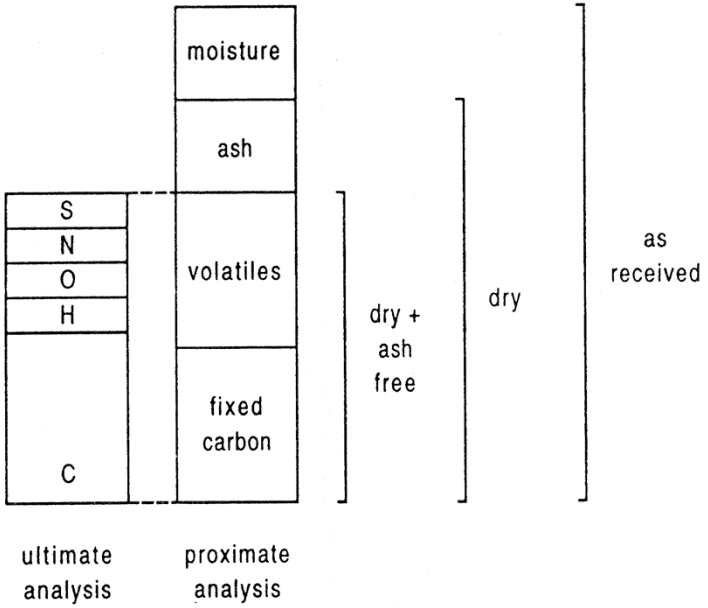

Figure 5.1: Coal composition by proximate and ultimate analysis

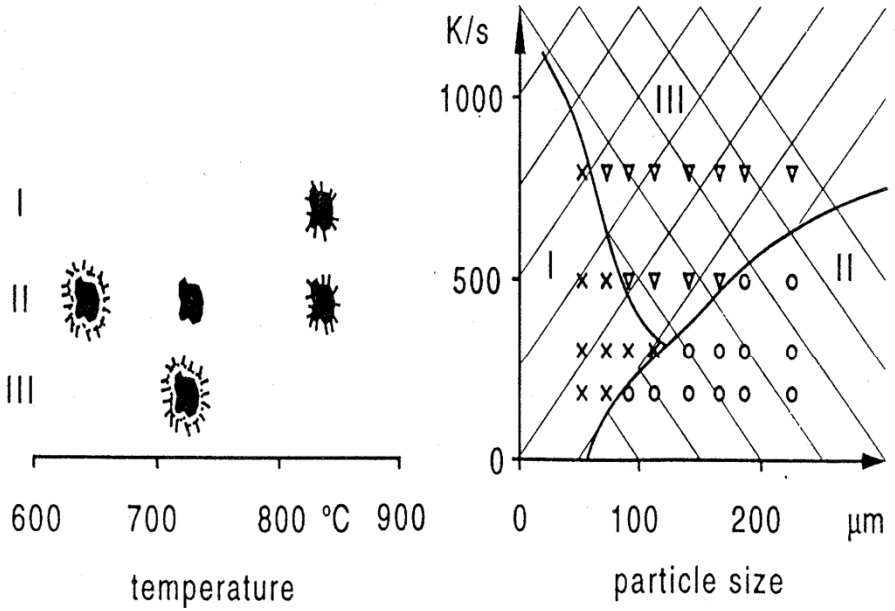

Figure 5.3: Ignition mechanisms at a coal particle after Stahlherm et al. (1974)
I: Particle ignition and volatile combustion
II: 1. Volatile ignition and combustion, 2. Heat up, 3. Particle ignition
III: Parallel ignition of volatiles and particle
×, o, ∇: Optical measurements

In fluidized beds all three mechanisms occur due to wide particle size ranges and high heating rates. It is up to the detailed models concerning drying, devolatilization and char combustion to consider the different effects in the proper quantities.

Devolatilization of Coal (석탄의 열분해)

석탄변환공정에서 초기단계로서, 70%까지의 석탄의 질량감소를 야기시키고, 50%까지의 열량을 기여한다.

휘발분의 수율은 석탄내 휘발분의 양에 좌우되며, 열분해 온도와 가열속도 등에 크게 좌우된다.

유동층에서 석탄의 가열속도는 약 10^4 K/sec .

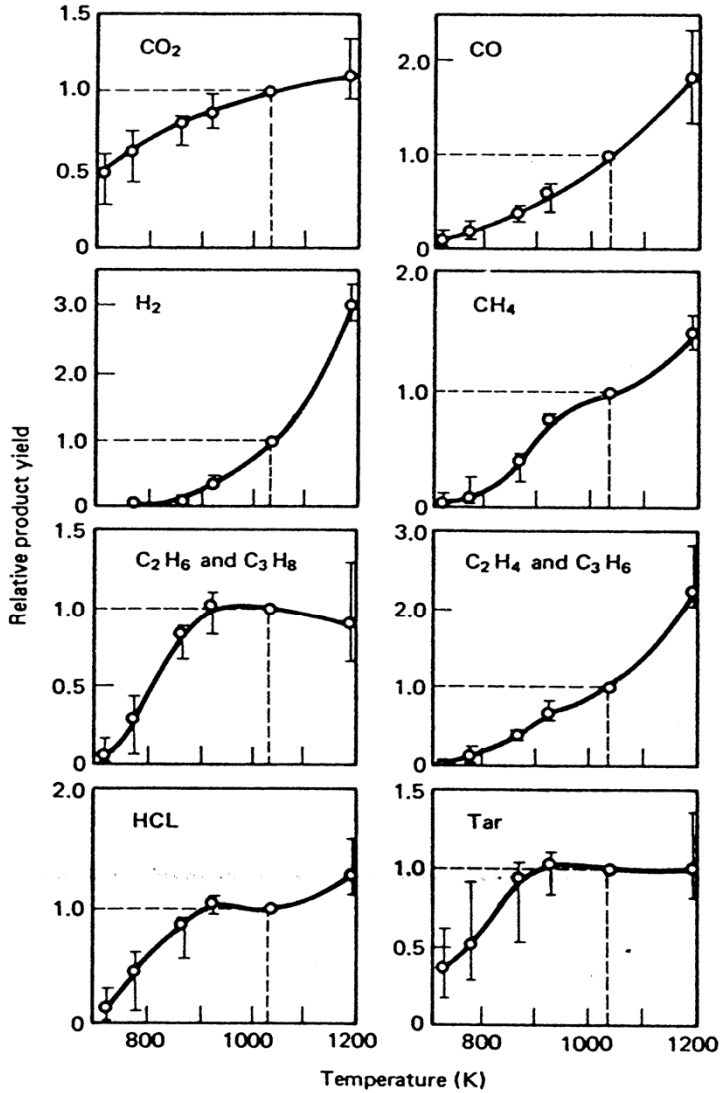

Figure 1 Unified temperature profile for the yields of various products upon flash pyrolysis in Ar. Relative product yield against the yield at 1037 K is presented. Circles and bars indicate the median and the range of the ratios for the 7 coals

from Xu and Tomita (1987), Fuel, 66, 632

열분해생성물의 예측

Temperature dependence of tar composition (Goyal and Rehmat, 1993)

$$X_{tar} = -4.95\times10^{-4}T + 77.4\times10^{-2} \quad (1)$$

$$X_H = -2.41\times10^{-4}T + 40.23\times10^{-2}$$

$$X_O = -2.25\times10^{-4}T + 30.74\times10^{-2} \qquad T \le 1077\,\mathrm{K}$$

$$X_O = 6.5\times10^{-2} \qquad 1077 < T \le 1144\ \mathrm{K}$$

$$X_N = -1.51\times10^{-4}T + 28.44\times10^{-2}$$

$$X_S = -2.7\times10^{-4}T + 37.4\times10^{-2}$$

Assume that a certain fraction of tar undergoes partial combustion/ decomposition:

$$C_\nu H_\alpha O_\beta S_\gamma N_\delta + \frac{1}{2}[\nu - \beta]O_2 = \gamma H_2S + \delta NH_3 + \nu CO + \frac{1}{2}(\alpha - 2\gamma - 3\delta)H_2 \quad (2)$$

Gas yields

$$Y_{H_2O} = 0.375 \quad (3)$$

$$Y_{CO} = 0.283 \quad (4)$$

$$Y_{CO_2} = 0.167 - 0.0017\ /(\mathrm{O/C}) \quad (5)$$

$$H_{avail} = (\mathrm{H/C}) - 2(\mathrm{H_2O/C}) \quad (6)$$

$$Y_{CH_4} = 0.085\,H_{avail} + 7.65\times10^{-5}T - 0.1152 \quad (7)$$

$$Y_{NH_3} = 0.19$$

$$Y_{H_2S} = 3.91\times10^{-4}T - 0.106$$

$$Y_{COS} = 0.005$$

The hydrogen and nitrogen in the product can be determined by elemental balance.

Loison and Chauvin (1964) require only a proximate analysis of coal, but they do not account the temperature effects.

$$x_{H_2} = 0.157 - 0.868x_{MV} + 1.388x_{MV}^2$$
$$x_{CO} = 0.428 - 2.653x_{MV} + 4.845x_{MV}^2$$
$$x_{H_2O} = 0.409 - 2.389x_{MV} + 4.554x_{MV}^2$$
$$x_{CH_4} = 0.201 - 0.469x_{MV} + 0.241x_{MV}^2$$
$$x_{CO_2} = 0.135 - 0.900x_{MV} + 1.906x_{MV}^2$$
$$x_{tar} = -0.325 + 7.279x_{MV} - 12.880x_{MV}^2$$

where, x_{MV} = the mass fraction of volatile matter in coal on a dry and ash-free basis, x_i = mass fraction of component *i* in the products of pyrolysis, kg/kg

Ma et al. (1989) correlated the various gas yields in devolatilization of sub-bituminous coal and lignite in a pilot-scale coal gasifier

$$M_i / M_{daf} = A_i + B_i T \qquad (8)$$

Lee at al. (1997) and Kim (2000) measured the product gases in relatively large fluidized beds and correlated their gas yields as a function of temperature as like equation (8).

Goyal and Rehmat (1993) may be used to predict variables in devolatilization stage in a coal gasification process.

A result

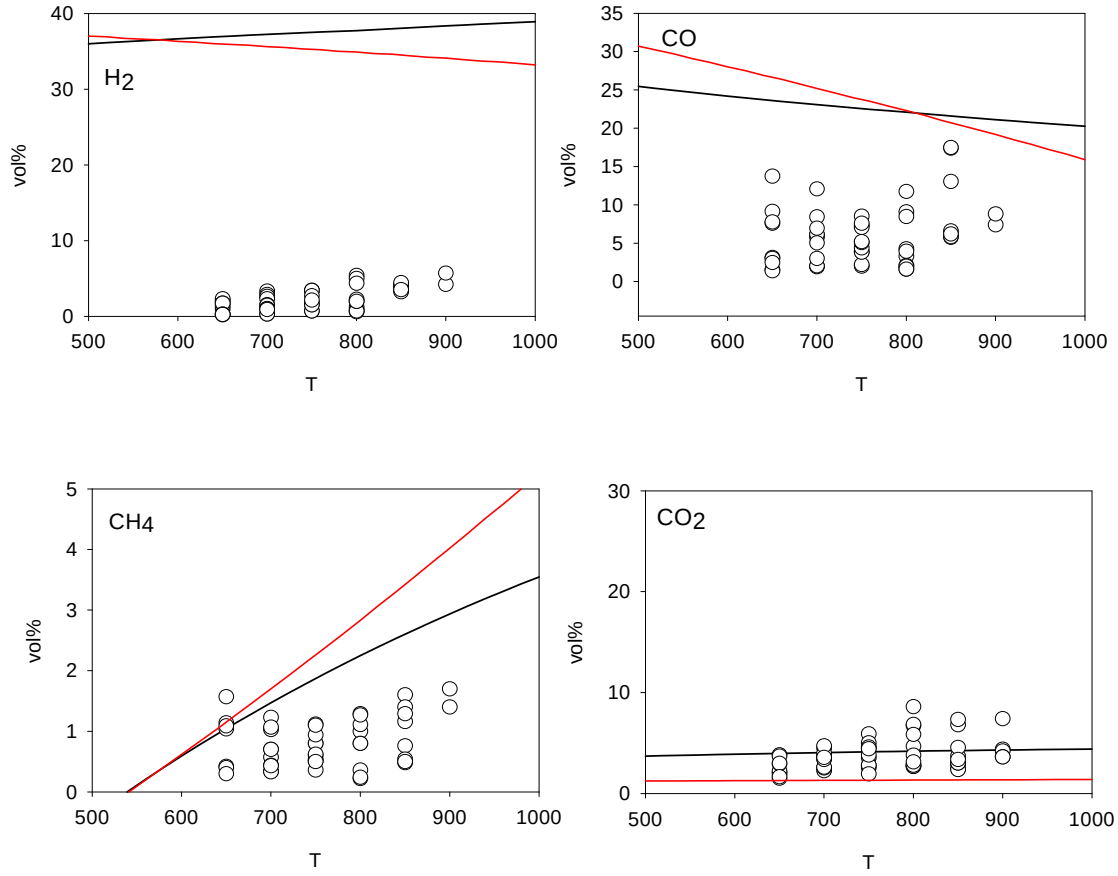

Fig. 2. Comparison of the predicted and experimental data for the gas yields from devolatilization of Australian subituminous coal (red = Goyal & Rehmat; black = Tsuiji & Watkinson's relation, coal feed = 1.5 kg/h, nitrogen feed = 50 vol.%)

Combustion of char

C + O2 = CO2 (a)
C + 1/2 O2 = CO (b)
C + CO2 = 2CO (c)
CO +1/2 O2 = CO2 (d)

Single film theory (Direct oxidation model) for small particles.
Both (a) and (b) occur at char surface.
The rate of (c) is very low, so can be neglected.
Some of CO oxidizes to CO2 by (d).

CO의 연소는 어디에서 일어나는가?
1mm 이상의 큰 입자인 경우 CO 는 서서히 확산되어나와서 입자표면 근처에서 타게된다. 반면 작은 입자의 경우에는 CO가 재빨리 확산되어 나온다 (Ross & Davidson, 1981)

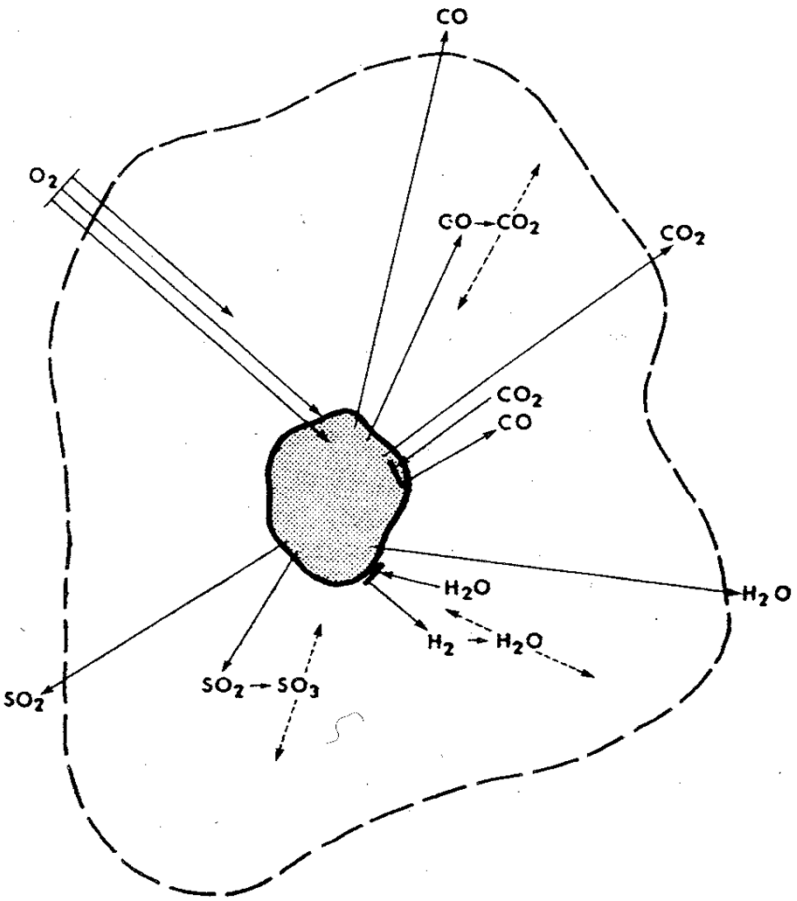

Fig. 10.1.1 Oxidation reactions in and near a burning char particle.

The effective reaction at the char surface:

$$C + \frac{1}{\Phi} O_2 = \left(2 - \frac{2}{\Phi}\right) CO + \left(\frac{2}{\Phi} - 1\right) CO_2$$

Φ = 1 for CO2 transport from the surface, 2 for CO transport.
The mechanism factor depends on diameter and temperature.

$$\Phi = \frac{2p+2}{p+2} \qquad d \le 0.05\times10^{-3}\, m$$

$$\Phi = \frac{2p+2-p(100d-0.005)/0.095}{p+2} \qquad 0.05\times10^{-3}\, m \le d \le 1\times10^{-3}\, m$$

$$\Phi = 1 \qquad d > 1\times10^{-3}\, m$$

The ratio of CO to CO2 formed at the char surface

$$p = 2500 \exp\left(\frac{-6244}{T}\right)$$

How is the rate expression ?

Carbon combustion rate of a particle can be defined as

$$r_C = \pi d^2 k_C C_{Ae} \qquad (3.2\text{-}12)$$

where

$$k_C = \frac{1}{\frac{1}{k_S} + \frac{1}{\Phi k_{diff}}}$$

Specific carbon combustion rate is by dividing (3.2-12) with particle volume.

$$r_{Char} = \frac{6}{d} k_C C_{O_2}$$

The mass transfer coefficient is given by

$$k_{diff} = Sh \cdot \frac{D_g}{d}$$

For a single particle in a gas flow

$$Sh = 2 + 0.69\,\mathrm{Re}^{1/2}\,Sc^{1/3}$$

Chakrabourty and Howard (1981) considered fluidization state,

$$Sh = 2 \cdot \varepsilon + 0.69 S_C^{1/3}\,\mathrm{Re}^{1/2} \qquad \text{where ,} \quad \mathrm{Re} = \frac{\rho_g U_t d}{\mu_g} \quad Sc = \frac{\nu_g}{D_g}$$

Diffusivity of oxygen at nitrogen atmosphere

$$D_g = 8.34 \times 10^{-4} T^{1.75} \frac{1}{P}$$

As pressure increases,

$$r_{O2} = \frac{P}{aP^n + b}$$

Combustion Kinetics on the char surface

$$k_S = k_0 \exp\left(-\frac{E}{RT_P}\right)$$

Smith (1978) suggested n = 1 for T>1000 K and n = 0.5 for T<1000 K
Let's set n = 1 refer to literature data of Table 5.1

$$k_S = 595\ T_P \exp\left(-\frac{149200}{RT_P}\right)$$

reference	carbon density $[\frac{kg}{m^3}]$	$k^*_{reac,0}\ [\frac{kg}{m^2 s (kPa)^n}]$	E/R_G [K]	reaction order n	fuel
Hamor et al. (1973)	440	0.918	8200	0.5	Brown coal char
Goldman et al. (1984)	1500	790	17676	1.0	Anthracite char
Smith (1970)	1500	1.90	9561	1	Anthracite char
Smith (1971a)	1360	2.013	9600	1.0	Semi-anthracite
Smith and Tyler (1972)	1320	5.428	20100	1.0	Semi-anthracite char
Sergant and Smith (1973)	760	2.902	10300	1.0	Bituminous char
Howard and Essenhigh (1967)	-	-	3000 - 6000	1.0	Bituminous char
Daw and Krishnan (1983)	-	0.0404	5787	0.6	Illinois coal (Bit.)
Song and Basu (1991)	-	20.57	9600	0.5	Prince coal (Bit.) (T_s < 1000 K)
Song and Basu (1991)	-	0.0263	3106	0.5	Prince coal (Bit.) (T_s > 1000 K)
Young and Smith (1981)	1640 - 1850	7.0	9911	0.5	Petroleum coke
Field et al. (1967)	-	859.0	17976	1.0	Various char
Smith (1971b)	1640 - 1850	1.97	9058	1	Petroleum coke
Smith (1971b)	1500	0.99	8555	1	Anthracite char
Smith (1971b)	470 - 7900	0.79	8052	1	Bituminous char
Halder and Basu (1987)	1640	1.10	8125	0.4	Electrode carbon
Essenhigh et al. (1965)	-	-	20000	0	T_s < 1000 K Carbon
				1.0	T_s > 1000 K

Table 5.1: Reactivities of various fuel particles, Basu and Fraser (1991)

Oxidation of combustion products

$$CO+\frac{1}{2}O_2=CO_2 \qquad \text{(d)}$$

Reaction (d) is strongly influenced by water conc.

$$r_{CO}=K_{CO}C_{CO}^{\alpha}C_{O_2}^{\beta}C_{H_2O}^{\gamma}$$

with $K_{CO}=6.5\times10^{10}\exp(-15100/T)$

Howard et al. (1973): α=1, β=0.5, γ=0.5

Author	K_0 $\frac{(mol/m^3)^n}{s}$	E/R (K)	α (–)	β (–)	γ (–)	ϑ (°C)	p (bar)
Howard et al. (1973)	1.310^8	15106	1	0.5	0.5	567 ... 2087	
Hottel et al. (1965)	1.910^6	8056	1	0.3	0.5	977 ... 1277	0.25-1
Dryer et al. (1973)	1.310^{10}	20141	1	0.25	0.5	977 ... 1277	1
Yetter et al. (1986)	7.210^{14}	34743	1	0.25	0.5	977 ... 1277	0.3-3
Lyon et al. (1985)	4.710^5	11883	1	0.25	0.5	977 ... 1277	1
Lavrov (1968)	5.710^7	14250	1	0.25	0.5	977 ... 1277	1
Hayhurst et al. (1990)	$1.817^{0.5}$	-	1	0.5	-	977 ... 1277	1
Schöler (1992)	1.4310^4	6699	1	0.5	0.5	-	1
This work	1.10^7	15106	1	0.5	0.5	-	

Table 5.3: Approaches for the homogeneous oxidation of CO (with $n = 1-\alpha-\beta-\gamma$), partially assembled by Braun (1996)

To get combustion rate of a single particle, It is necessary to know oxygen concentration in the surrounding emulsion phase. → This leads us to the fluid mechanics and gas mixing of a fluidized bed.

3.3 Fluidization & Mixing

Highly expanded bed $\varepsilon > 0.65$ → CFB (순환유동층)
Beds with $0.45 < \varepsilon < 0.65$ → Bubbling FB

Two-phase theory (Toomey & Johnstone, 1952).
The gas is thought to percolate through two regions:
Bubble phase and emulsion phase.
The two phases being interconnected by mass transfer

Flow regimes.

regime	characteristics	criterion
fixed	-gas percolates through the voids between the stationary particle	$U < U_{mf}$
slow bubble	-interstitial gas velocity (I.e. velocity of the gas percolating through the emulsion phase) -part of the interstitial gas uses bubble as shortcut	$u_e > u_{br}$
fast bubble	-interstitial gas velocity is below the rising velocity of bubbles -circulation gas flow in bubbles gives rise to cloud region	$u_e < u_{br}$
rapidly growing bubble region,	-bubble growth rate exceeds bubble rise velocity	$\frac{d(d_b)}{d_t} > u_{br}$
apparent slugging	-gas accumulation in bubbles is of same order as through flow	
turbulent regime	-turbulent flow with small flow channels -vigorous circulation of the solids in the bed	$U = 0.5\, U_t$
pneumatic transport	-complete elutriation of bed mass	$U > U_t$

Most modeling work is fast bubble regime, dominant in small particle systems.
Gas mixing differs substantially for each regimes. In fast bubble regime the circulating gas flow in the bubbles gives rise to a substantial resistance to mass transfer between the two phases, → very important !

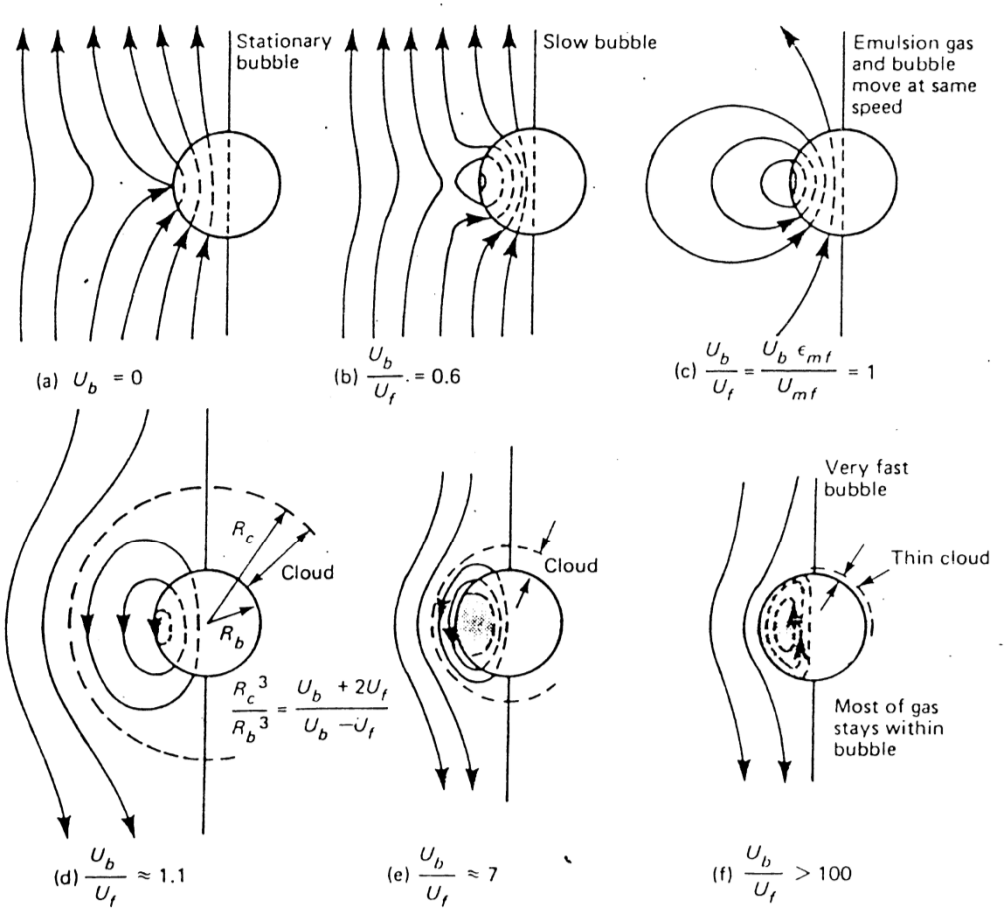

Figure 1.10 Streamlines of gas near a single rising bubble, from the Davidson model. Only flow on the left side is shown; the right side is symmetric (From Kunii and Levenspiel[31])

Fluid Dynamics

- Minimum fluidization velocity.

Ergun (1952) used frictional pressure drop balance and suggested:

$$\frac{1.75}{\varepsilon_{mf}^3 \Phi_s} \mathrm{Re}_{mf}^2 + \frac{150(1-\varepsilon_{mf})}{\varepsilon_{mf}^3 {\Phi_s}^2} \mathrm{Re}_{mf} = Ar$$

Containing the minimum fluidization velocity in the Reynolds number

$$\mathrm{Re}_{mf} = \frac{U_{mf} d_s \rho_g}{\mu_g}$$

and the solid and gas properties in the Archimedes number

$$Ar = \frac{d_s^3 \rho_g (\rho_s - \rho_g) g}{\mu_g^2}$$

A different approach was suggested by Broadhurst and Becker(1975)

$$\frac{Ar}{\mathrm{Re}_{mf}^2} = K_1 \left(\frac{\rho_g}{\rho_s} \right)^{0.22} Ar^{-0.82} + K_2$$

The correlation of Wen & Yu(1966) which does not require a particle shape fa

$$\mathrm{Re}_{mf} = \left(33.7^2 + 0.0408 Ar\right)^{0.5} - 33.7 \qquad (3.3\text{-}1)$$

gives a decreasing U_{mf} with higher T, P

The bed voidage at minimum fluidization state. Broadhurst and Becker(1975)

$$\varepsilon_{mf} = 0.586 \Phi^{-0.72} Ar^{-0.029} \left(\frac{\rho_g}{\rho_s} \right)^{0.021}$$

for the ranges $0.85 < \Phi < 1$, $1 < Ar < 100000$ and $500 < \rho_s / \rho_g < 50000$.

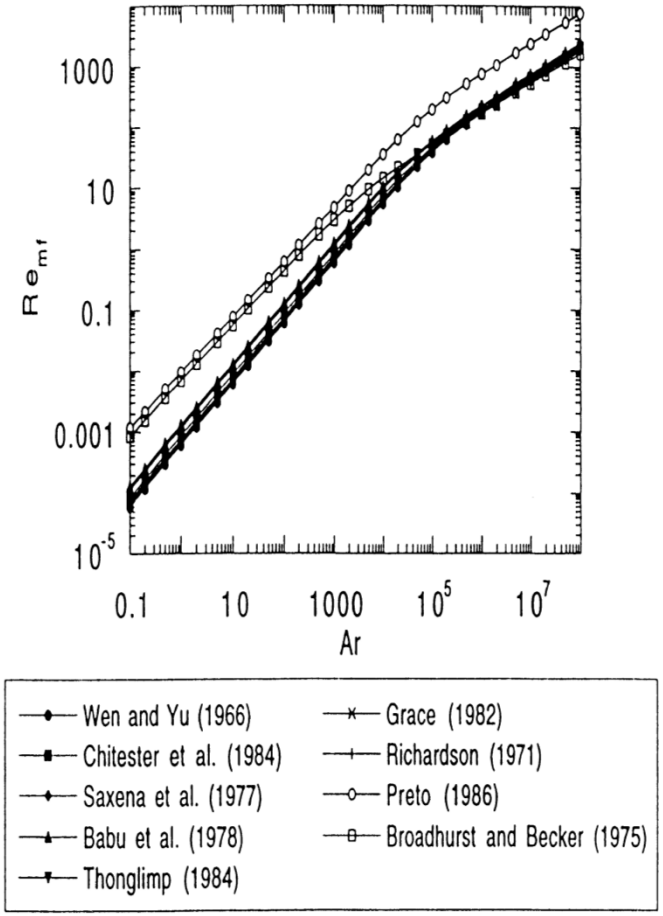

Figure 4.8: Comparison of approaches for minimum fluidization state

Two-phase flow division

주입된 가스가 two phase로 분산되는 정도와 two-phase 간의 물질전달은 고체입자와 접촉하는 가스의 양을 결정한다.
결국 석탄입자로 공급되는 산소의 양과 석탄입자로부터의 제거되는 열량을 결정하게 되므로 중요하다.

최소유동화에 요구되는 양을 넘는 과량의 가스는 bubble의 형태로 흐른다.

$$Q_T = Q_b + Q_{mf}$$

윗 식을 층면적으로 나누면, 소위 *visible bubble flow* 이다,

$$\frac{Q_b}{A} = U - U_{mf}$$

실험적인 증거에 의하면 two-phase theory 는 visible bubble flow를 과대하게 예측하고 있다.
즉, 실제로는 더 많은 가스가 emulsion 으로 흐른다.

$$\frac{Q_b}{A} = U - U_{mf}(1 + n\delta)$$

δ is the volume fraction of bubbles in the bed.
n = 0 means ‘ ideal’ two-phase theory.
larger n → emulsion phase flow is larger, the departure from ideality becomes greater.

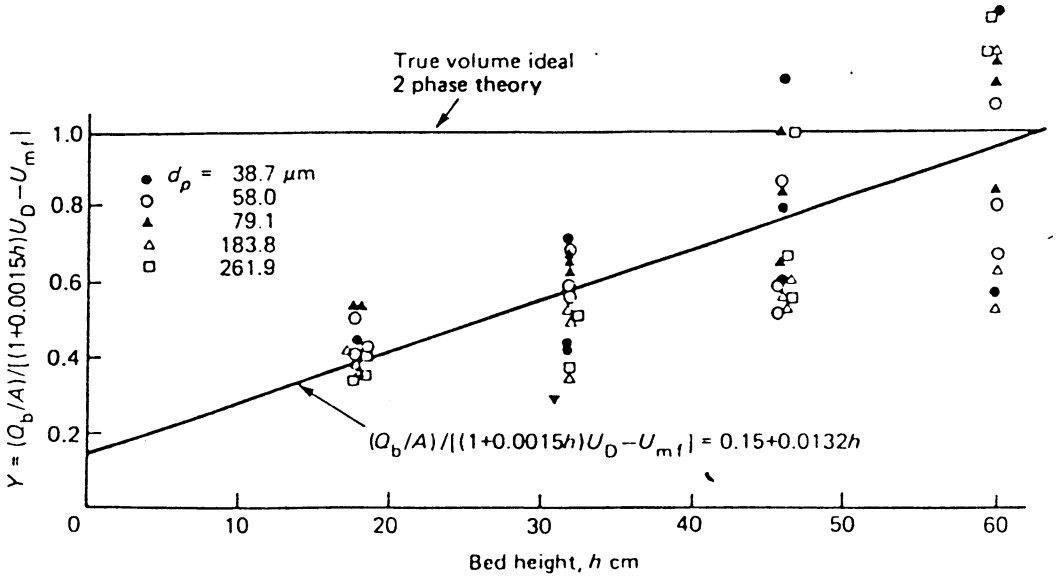

Figure 1.5 Variation of the expectation of the ideal true volume two-phase theory with bed height (From Rowe and Yacono[27])

Another way,

$$\frac{Q_b}{A} = \gamma(U - U_{mf}), \qquad 0 < \gamma \leq 1$$

author	γ	Remarks
Cranfield, Geldart(1974)	0.55	dp = 1000 – 2000 um
Xavier et al.(1978)	0.8	dp = 158 – 885 um
Subzwari et al.(1978)	0.6 – 0.9	dp = 100u. γ decreasing with P

Correlations on Bubble Diameter

Yasui and Johanson(1958)

$$L_v = 0.33\rho_s d_p \left[\left(U_g - U_{mf}\right) - 1\right]^{0.63} H$$

Geldart(1972)

$$D_e = \frac{1.43}{g^{0.2}}\left[\frac{\left(U_g - U_{mf}\right)D^2}{4N_{or}}\right]^{0.4} + 2.05\left(U_g - U_{mf}\right)^{0.94} H$$

Mori and Wen(1975)

$$\frac{D_{bm} - D_e}{D_{bm} - D_{bo}} = \exp\left[-0.3H / D_c\right]$$

$$D_{bm} = 2.59 g^{0.2}\left[\left(U_g - U_{mf}\right) / A_t\right]^{0.4}$$

$$D_{bo} = 1.38 g^{0.2}\left[\left(A_t / N_{or}\right)\left(U_g - U_{mf}\right)\right]^{0.4}$$

Rowe(1976)

$$D_e = \left(U_g - U_{mf}\right)^{1/2}(H + H_0)^{3/4} / g^{1/4}$$

Wether(1976)

$$D_e = 0.00853\left[1 + 27.2\left(U_g - U_{mf}\right)\right]^{1/3}\left(1 + 6.84H\right)^{1.21}$$

Darton et al.(1977)

$$D_e = 0.54\left(U_g - U_{mf}\right)^{0.4}\left(H + 2\sqrt{\pi} d_{or}\right)^{0.8} / g^{0.2}$$

Choi et al.(1988)

$$D_e = 1.787\left(U_g - U_{mf}\right)^{2/3}\left\{H + 0.419 g^{1/2} D_e{}^{3/2} / \left(U_g - U_{mf}\right)\right\}^{2/3} / g^{1/3}$$

Bubble size

대부분의 상관식은 small particle systems에서 유도되었는데, Glicksman et al.(1981) 에 의하면
이러한 상관식은 큰 입자의 경우에 기포의 크기를 실제보다 작게 예측하고 있다.

No correlations to dat for the influence of bed internals – Heat exchanger tubes.

A mechanistic model of bubble coalescence was proposed by Darton et al. (1977) which leads to an equation predicting bubble diameter closely similar to those resulting from empirical studies. Assuming the two-phase theory to apply, the variation of bubble diameter with height is calculated to be:

$$d_b = \frac{0.54(U - U_{mf})^{0.4}(z + 4\sqrt{A_0})^{0.8}}{g^{0.2}}$$ in SI unit.

where A_0 is the so-called ' catchment area' which is taken to be the area of distributor per orifice; zero for a porous plate distributor.

In accordance with the analysis of Bar- Cohen et al.(1981) of the data at large particles.

$$d_b = \alpha(U - U_{mf})z^{0.75}$$

with α a parameter.

Bubbles velocity

On the basis of two-phase theory, Davidson & Harrison (1963) proposed the rise velocities.
For single bubble.

$$U_{br} = 0.711\sqrt{gd_b}$$

For bubbles in bubbling beds:

$$\boxed{U_b = (U - U_{mf}) + 0.711\sqrt{gd_b}}$$

Weimer & Clough(1983).

$$\boxed{U_b = C_D \frac{Q_b}{A} + 0.71\left[\frac{gd_b(\rho_s - \rho_g)(1-\delta)}{\rho_s}\right]^{0.5}} \qquad (3.3\text{-}9)$$

with C_D is the distribution coefficient for bubbles over the bed cross section.

Bed height (or expansion)

Bed mass from mass balance

$$M_s = \rho_s \int_0^{H_B} A(z)[1 - \varepsilon(z)]dz$$

where bed voidage is given by

$$\varepsilon(z) = \delta(z) + [1 - \delta(z)]\varepsilon_{mf}$$

the local bubble fraction δ (z) is related to the visible bubble flow ;

$$\delta(z) = \frac{Q_b / A}{U_b(z)}$$

Kunii and Levenspiel (1991)

$$\delta = \frac{U - U_{mf}}{U_B}$$

Mixing

Solid mixing

기포가 상승하면서 고체를 뒤섞는 관계로 고체의 수직방향 혼합은 활발하다. 그러나 측면의 혼합은 상대적으로 order 가 적다. 측면혼합은 보통 diffusion equation 으로 묘사한다 (Highley & Merrick, 1971; Tojo et al, 1981).

그러나 유동층의 단면적이 비교적 작은 경우에는 emulsion phase 를 완전혼합조건으로 가정할 수 있다.

Gas mixing

기체-고체 반응에 그 영향이 매우 크다. 가스의 혼합특성은 flow regime 에 따라 큰 차이를 나타낸다.

Slow-bubble regime 에서는 많은 양의 emulsion gas 가 기포를 통해 흘러간다. 결국 거의 plug flow 조건으로 본다.

Fast-bubble regime 에서는 기포를 통과하는 가스흐름이 무척 적어져서, bubble 과 emulsion 상은 뚜렷하게 구분된다.

Neglecting radial relations and excluding the chemical reactions,
the gas mass balances for bubble phase are;

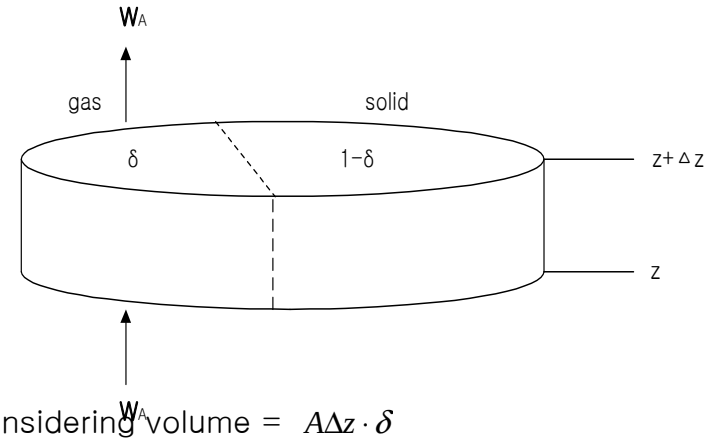

considering volume = $A\Delta z \cdot \delta$

Mol flux = 농도구배로 인한 Molecules diffusion flux + 유체의 운동으로 인한 bulk flux

$$W_A = -D_{AB}\nabla C_A + C_A \bar{u}$$

ACC = in − out

$$A\Delta z\delta\frac{\partial C_b}{\partial t} = W_A \cdot A\delta|_z - W_A \cdot A\delta|_{z+\Delta z} - (A\Delta z\delta)K_{be}(C_b - C_e)$$

양변을 $A\Delta z \cdot \delta$ 으로 나눈후 $\Delta z \to 0$ 로 보내면,

$$\therefore \delta\frac{\partial C_b}{\partial t} = \delta D_b\frac{\partial^2 C_b}{\partial z^2} - \frac{Q_b}{A}\frac{\partial C_b}{\partial z} - \delta K_{be}(C_b - C_e) \qquad (3.3\text{-}14)$$

the gas mass balances for emulsion phase are;

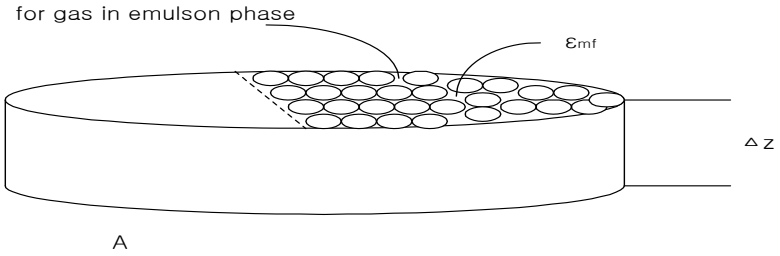

considering volume = $A\Delta z \cdot (1-\delta)\varepsilon_{mf}$

As like before,

$$(1-\delta)\varepsilon_{mf}\frac{\partial C_e}{\partial t} = (1-\delta)\varepsilon_{mf}\cdot D_e\frac{\partial^2 C_e}{\partial z^2} - \frac{Q_e}{A}\frac{\partial C_e}{\partial z} + (1-\delta)\varepsilon_{mf}K_{be}(C_b - C_e) \quad (3.3\text{-}15)$$

Simplifying assumptions:

The gas in bubble phase is almost treated to be in plug flow, i.e. $D_b=0$

How about the emulsion phase gas?

- -plug flow (De=0) : upward or downward flow
- -complete mixing (De=∞)

Mixing phenomena may be considered to be in steady state. Eq(3.3-14) & (3.3-15) then reduce to;

$$\frac{Q_b}{A}\frac{dC_b}{dz} = -\delta K_{be}(C_b - C_e) \quad (16)$$

for the emulsion phase in plug flow,

$$\frac{Q_b}{A}\frac{dC_b}{dz} = (1-\delta)\varepsilon_{mf}\cdot K_{be}(C_b - C_{e)}) \quad (17)$$

for the completely mixed emulsion phase,

$$\frac{Q_e}{A}(C_o - C_e) + \int_0^{H_B}\delta K_{be}(C_b - C_e)dz = 0 \quad (18)$$

Gas interchange between bubble and emulsion phase.

(i) diffusive mechanism : like a gas bubble in a liquid.
(ii) convective process : is due to the gas " through flow" through the bubble surface.

Slow bubble의 경우는 emulsion과 충분한 가스교환이 이루어져서 두 상사이에 가스농도 차이가 거의 없다고 본다. Fast bubble은 가스의 바이패스가 있어서 농도차이가 있다.

The gas interchange coefficient from Kobayashi et al.[1967]

$$K_{be} = \frac{0.11}{d_b}$$

Kunii and Levenspiel (1977)

$$K_{be} = \frac{1}{1/K_1 + 1/K_2}$$

where

$$K_1 = 4.5\frac{U_{mf}}{d_b} + 5.85\frac{D_g^{0.5} g^{0.25}}{d_b^{1.25}}$$

$$K_2 = 6.78\sqrt{\frac{\varepsilon_{mf} D_g U_b}{d_b^3}}$$

Davidson & Harrison(1963) derive the following on theoretic grounds;

$$K_{be} = 4.5\frac{U_{mf}}{d_b} + 10.35\left[\frac{D_g}{d_b^{2.5}}\right]^{0.5} \qquad (19)$$

Sit & Grace(1981) propose to account for bubble interactions:

$$K_{be} = 2.0\frac{U_{mf}}{d_b} + 6.77\left[\frac{D_g \cdot \varepsilon_{mf} u_b}{d_b^3}\right]^{0.5} \qquad (20)$$

convective contribution　　diffusive contribution

Good reference: a compilation of Sit & Grace(1978).

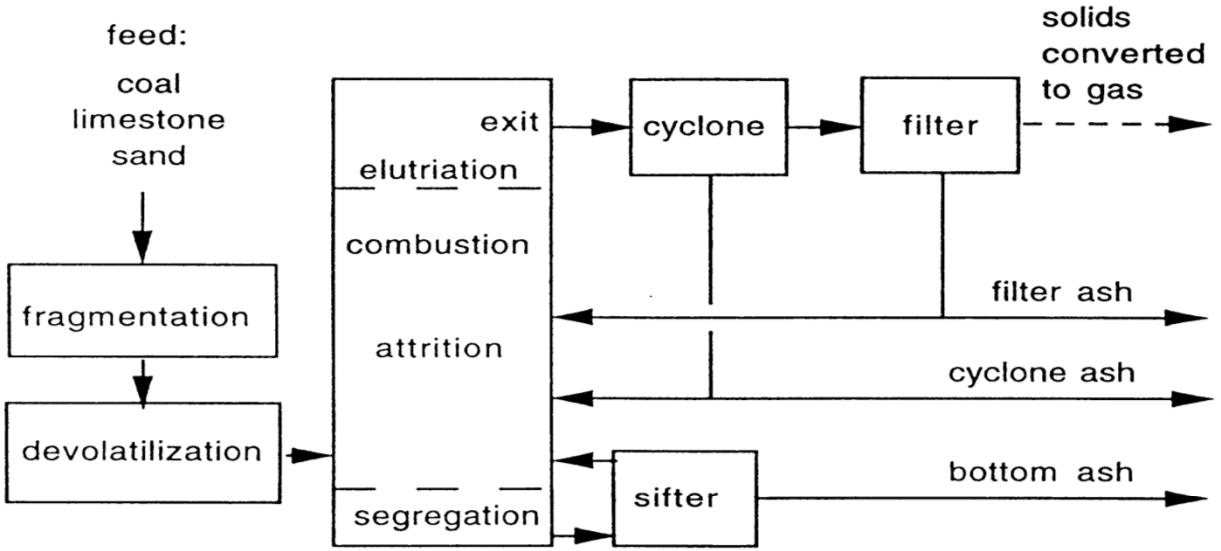

Figure 4.19: Overall balance of solids

- Elutriation: Particles are blown up in the riser and leave it as they pass the exit which creates a separation effect
- Cyclone: The particles are separated from the gas, a small amount of fines escapes the system and is captured in the filter, the rest is fed back
- Segregation: Coarse particles accumulate at the bottom where they are extracted to keep the mass inventory constant. Some systems have a wind sifter to return the smaller particles, or an ash mill to grind the returned ash

Shrinking rate of a char particle [m/s] is found by additive contributions due to combustion and attrition:

$$S(d) = \frac{dd}{dt} = \left(\frac{dd}{dt}\right)_a + \left(\frac{dd}{dt}\right)_c \qquad (2\text{-}1)$$

The shrinkage due to combustion could be obtained from carbon balance for a particle.

$$\begin{pmatrix}\text{accumulation}\\ \text{of carbon within}\\ \text{a char particle}\end{pmatrix} = -\begin{pmatrix}\text{consumption}\\ \text{by}\\ \text{combustion}\end{pmatrix}$$

As the combustion rate of a char particle is

$$r_C = \pi d^2 k_C C_{O2,e} \qquad (2\text{-}2)$$

$$\frac{\partial}{\partial t}\left[\rho_{ch}\frac{w_{fc}}{w_{fc}+w_{as}}\cdot\frac{\pi}{6}d^3\cdot\frac{1}{M_C}\right] = -\pi d^2 k_C(d) C_{O2,e} \qquad (2\text{-}3)$$

Let $\beta = \dfrac{w_{fc}}{w_{fc}+w_{as}}$: fraction of fixed carbon in the char.

This yields:

$$\left(\frac{\partial d}{\partial t}\right)_C = -\frac{2M_C}{\rho_{ch}\beta}\cdot k_C(d) C_{O2,e} \qquad (2\text{-}4)$$

The oxygen conc. will be height-dependent. For easy solving, we can assume that $k_C(d)$ may be evaluated using the mean oxygen conc. in the emulsion phase, given by

$$\overline{C}_{O2,e} = \int_0^{H_B} a(z) C_{O2,e}(z) \cdot dz \qquad (2\text{-}5)$$

where

$$a(z) = \frac{[1-\delta(z)]A_B(z)}{\int_0^{H_B}[1-\delta(z)]A_B(z)\cdot dz}$$

The mean shrinking rate for char with diameter d is

$$\left(\frac{\partial d}{\partial t}\right)_C = -\frac{2M_C}{\rho_{ch}\beta}\cdot k_C(d)\overline{C}_{O2,e} \qquad (2\text{-}9)$$

where kc is the overall rate constant and is given by

$$k_C = \frac{1}{\frac{1}{k_S}+\frac{1}{k_{diff}}} \qquad (2\text{-}11)$$

$$k_S = 595T\exp\left[-\frac{149200}{RT}\right]f_r \qquad \text{where R = 8.314 J/mol.K} \qquad (2\text{-}12)$$

Attrition Models

For combustion-assisted attrition,

Mass rate of carbon fines elutriated is proportional to the carbon surface exposed to attrition. (Donsi et al., 1981)

$$E_a = K(U - U_{mf})\left(\frac{M_b}{d}\right) \qquad (3\text{-}1)$$ for lager size than inert

Merrick & Highley (1974)는 석탄회재 및 dolomite로 이루어진 유동층의 elutriation 거동을 조사하였다. 미세분의 생성속도는 Umf 이상의 excess gas velocity 와 층무게에 비례한다고 제시하였다.

$$E_a = K(U - U_{mf})M_b \qquad (3\text{-}2)$$ for same size as inert

When Eq.(3-2) applied to each size range of particles,

$$-E_{ax} = \frac{dM_x}{dt} = -K(U - U_{mf})M_x \qquad (3\text{-}4)$$

where M_x = weight of particles of mean size x in the bed.

Then the rate of size reduction is,

$$\left(\frac{dd}{dt}\right)_a = -\frac{K}{3}(U - U_{mf})d \qquad (3\text{-}5)$$

실험에 의하면 큰입자들은 식 (3-4)의 예측보다 더 빨리 마모되어진다. 미세한 입자들이 큰입자들 사이의 공간에서 어느정도 시간을 보내기 때문이다. 이 시간은 자기보다 큰 voids 에 비례할 것이다. 따라서 하나의 보정인자를 도입할 수 있다.

$$\left(\frac{dd}{dt}\right)_a = -\frac{K}{3} f_x(U - U_{mf})d \qquad (3\text{-}7)$$ used in IEA CFBC MODEL

where f_x = fraction of particles in the bed smaller than size d.

The attrition constant(마모상수) K 는 석탄의 종류, 연소로의 형태, 크기에 따라 좌우될수 있는데, 이러한 영향을 고려하기 위해서는 아직도 부가적인 실험들이 필요하다.

Massimilla and Salatino(1987) proposed the constant in Donsi' s.

$$K = K_0 \frac{\rho_p d_p (1 - X) g}{\phi_v(X)} \qquad (3\text{-}9)$$

where

ρ_p, d_p : the density and diameter of bed inert particles.

X : degree of carbon conversion.

ϕ_v : the deformation work per unit volume at the failure point of carbon.

But, the evaluation of ϕ_v is much more difficult !!!

Lin et al. (1980) in char/sand fluidized bed:

$$\left(\frac{dd}{dt}\right)_a = -a \exp\left[b(U - U_{mf})\right] d \qquad (3\text{-}10)$$

Lee and Keener (1993) at the attrition of lime sorbents in CFB Absorber.

$$\frac{dW}{dt} = -K_a \frac{(W^2 - W_{\min}^2)}{(U - U_{mf})^2} \qquad (3\text{-}11)$$

where $K_a = K_0 \exp\left[-\frac{E_a}{(U - U_{mf})^2}\right]$

W: weight of parent solids in the bed

Wmin: the minimum weight with which the attrition may be negligible after a long fluidization.

Ea : attrition activation energy.

Wells and Kriahnaa (CONF-800545-1) presented that the attrition is strongly influenced by the feed system design of the AFBC. For example, the series 5 data can be correlated by

$$E_a = 6.74 (d_{pf})^{0.5} U \tau^{1.224} \qquad (3\text{-}12)$$

E_a = rate of attrition, g/sec

d_{pf} = mean feed particle size distribution, cm

τ = weight space time (weight of bed/lime flow), hr.

Elutriation constant

The elutriation flux of particles size $\bar{d}$ is proportional to its weight fraction in the bed,

$$F_u[d \cdot d + \Delta d] = k_u(d)p(d)\Delta d$$

p(d) denoting the coal mass distribution
As another form:

$$\boxed{-\frac{1}{A_t}\frac{dW_i}{dt} = \kappa_i^*\left(\frac{W_i}{W}\right)}$$

Many correlations have been proposed for the elutriation rate constant $k_u(d)$, κ_i^* .

Merrick & Highley (1974)의 표현

$$F_u(d) = \frac{F_g}{M_B}\exp\left[-10.4\left(\frac{u_t}{u}\right)^{0.5}\left(\frac{u_{mf}}{u-u_{mf}}\right)^{0.25}\right] \qquad (3,4\text{-}4)$$

Where F_g the gas flow through the combustor and M_B the total bed mass.

TABLE 3 Correlations for Elutriation Rate Constant

Investigators	Experimental Conditions: d_t (m)	$d_{p,coarse}$ (μm)	d_{pi} (μm)	u_o (m/s)	Correlation, $Re_t = d_{pi}\rho_g u_{ti}/\mu$
Yagi and Aochi [25] (1955)	0.07–1.0	100–1600	80–300	0.3–1.0	$\frac{\kappa_i^* g d_{pi}^2}{\mu(u_o - u_{ti})^2} = 0.0015\,Re_t^{0.5} + 0.01\,Re_t^{1.2}$
Wen and Hashinger [26] (1960)	0.102	~710	50–150	0.61–0.98	$\frac{\kappa_i^*}{\rho_g(u_o - u_{ti})} = 1.52\times10^{-5}\frac{u_o - u_{ti}}{(g d_{pi})^{0.5}} \times Re_t^{0.725}\left(\frac{\rho_s - \rho_g}{\rho_g}\right)^{1.15}$
Tanaka et al. [27] (1972)	0.031–0.067	718–1930	106–505	0.9–2.8	$\frac{\kappa_i^*}{\rho_g(u_o - u_{ti})} = 0.046\frac{(u_o - u_{ti})}{(g d_{pi})^{0.5}} \times Re_t^{0.3}\left(\frac{\rho_s - \rho_g}{\rho_g}\right)^{0.15}$
Merrick and Highley [28] (1974)	0.91 × 0.91 0.91 × 0.46	63–1000	ash, 8–100	0.61–2.44	$\frac{\kappa_i^*}{\rho_g u_o} = 0.0001 + 130\exp\left[-10.4\left(\frac{u_{ti}}{u_o}\right)^{0.5}\left(\frac{u_{mf}}{u_o - u_{mf}}\right)^{0.25}\right]$
Geldart et al. [29] (1979)	0.076 0.30	60–350 ~1500	60–300	0.6–3	$\frac{\kappa_i^*}{\rho_g u_o} = 23.7\exp\left(-5.4\frac{u_{ti}}{u_o}\right)$
Colakyan and Levenspiel [30] (1984)	0.92 × 0.92 0.30 × 0.30	300–1000	36–542	0.901–3.66	$\kappa_i^* = 0.011\rho_s\left(1 - \frac{u_{ti}}{u_o}\right)^2, \quad \rho_s\ (kg/m^3)$
Kato et al. [6] (1986)	0.15 × 0.15	58–282	37–150	0.2–1.1	$\frac{\kappa_i^*}{\rho_g(u_o - u_{ti})} = 2.07\times10^{-4}\,Fr^{\alpha}\,Re_t^{1.6}\left(\frac{\rho_s - \rho_g}{\rho_g}\right)^{0.61}$ $\alpha = Re_t^{-0.6}$, $Fr = (u_o - u_{ti})^2/g d_{pi}$ for Geldart group **A** particles

SOLIDS POPULATION BALANCE

Levenspiel et al. [O.Levenspiel, D.Kunii and T. Fitzgerald. Powder Technol, 2, 87, (1968/69)] have derived a general equation for the solids balance around a fluidized bed reactor in which particle size changes because of reaction.

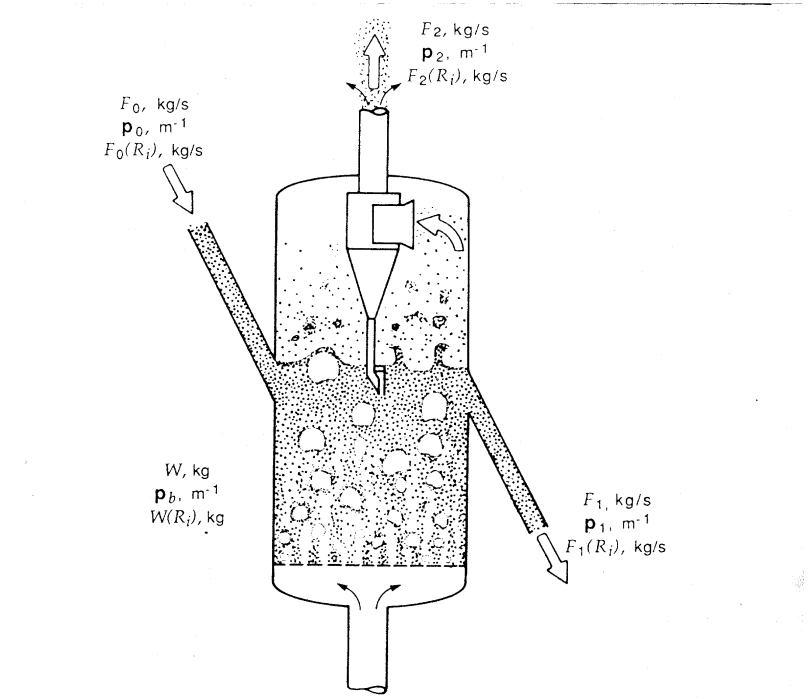

FIGURE 4
The fluidized bed operating with a wide size distribution of solids.

- Steady state
- Spherical particles of const density ρ_s.
- backmix flow in the bed (hence $p_b(R) = p_1(R)$
- particle growth or shrinkage given by a general $S(R)$

A balance for the solids contained in a cut of width ΔR can be written for growing particles as

$$\begin{pmatrix}\text{solids}\\ \text{entering in}\\ \text{feed}\end{pmatrix}-\begin{pmatrix}\text{solids}\\ \text{leaving in}\\ \text{overflow}\end{pmatrix}-\begin{pmatrix}\text{solids}\\ \text{leaving in}\\ \text{carryover}\end{pmatrix}+$$

$$\left[\begin{pmatrix}\text{solids growing into}\\ \text{the interval from}\\ \text{a smaller size}\end{pmatrix}-\begin{pmatrix}\text{solids growing}\\ \text{out of the interval}\\ \text{to a larger size}\end{pmatrix}\right]+\begin{pmatrix}\text{solids generation}\\ \text{due to growth}\\ \text{within interval}\end{pmatrix}=0$$

$$F_0 p_0(R)\Delta R - F_1 p_1(R)\Delta R - WK_e(R)p_1(R)\Delta R + Wp_1(R)S(R)\big|_R - Wp_1(R)S(R)\big|_{R+\Delta R} + \frac{3W}{R}p_1(R)S(R)\Delta R = 0 \quad (1)$$

from which,

A balance for the solids contained in a cut of width ΔR can be written for growing particles as

$$\begin{pmatrix}\text{solids}\\ \text{entering in}\\ \text{feed}\end{pmatrix}-\begin{pmatrix}\text{solids}\\ \text{leaving in}\\ \text{overflow}\end{pmatrix}-\begin{pmatrix}\text{solids}\\ \text{leaving in}\\ \text{carryover}\end{pmatrix}+$$

$$\left[\begin{pmatrix}\text{solids growing into}\\ \text{the interval from}\\ \text{a smaller size}\end{pmatrix}-\begin{pmatrix}\text{solids growing}\\ \text{out of the interval}\\ \text{to a larger size}\end{pmatrix}\right]+\begin{pmatrix}\text{solids generation}\\ \text{due to growth}\\ \text{within interval}\end{pmatrix}=0$$

$$F_0 p_0(R)\Delta R - F_1 p_1(R)\Delta R - WK_e(R)p_1(R)\Delta R + Wp_1(R)S(R)\big|_R - Wp_1(R)S(R)\big|_{R+\Delta R} + \frac{3W}{R}p_1(R)S(R)\Delta R = 0 \quad (1)$$

from which,

$$F_0 p_0(R) - F_1 p_1(R) - WK_e(R)p_1(R) - W\frac{d}{dR}[p_1(R)S(R)] + \frac{3W}{R}p_1(R)S(R) = 0 \quad (2)$$

same as equation (3.5-13) in Kool (1985)' s thesis (Dynamic model):

$$(w_{fc}+w_{as})\lambda_0(d,t) - k_u(d)\lambda(d,t) - \frac{\partial}{\partial t}[\lambda(d,t)S(d)] + \frac{3}{d}\lambda(d,t)S(d) = \frac{\partial}{\partial t}\lambda(d,t) \quad (3.5\text{-}13)$$

where $\lambda(d,t)$ [kg/m] denotes time-dependent mass distribution of char in the bed.

$p_1(R)$ [1/m] the size distribution function of char in the bed.

An overall mass balance represents the rate of generation or disappearance of all solids in the bed:

$$F_1 + F_2 - F_0 = \int_{\text{all R}} \frac{3\mathrm{W}p_b(R)S(R)}{R} dR \qquad < 0 \text{ for shrinkage.} \qquad (3)$$

The continuous size distributions of bed particles are given by

$$p_1(R) = \frac{F_0 R^3}{W|S(R)|} I(R, R_M) \int_R^{R_M} \frac{p_0(R_i)dR_i}{R_i^3 I(R_i, R_M)} \qquad (4)$$

where $$I(R, R_i) = \exp\left[-\int_{Ri}^{R} \frac{F_1/W + K_e(R)}{S(R)} dR \right] \qquad (5)$$

Overturf and Kayihan(Powder Technol.,23, 143-147, 1979) warn that taking the discrete size slices of the above equations may lead to very large errors unless many size slices are taken. They suggest a discrete from of equation (2)

For shrinking particles,

$$p_1(R_i) = \frac{F_0 p_0(R_i)\Delta R_i - W p_1(R_{i+1})S(R_{i+1})}{-WS(R_i) + F_1 \Delta R_i + WK_e(R_i)\Delta R_i - \frac{3W}{R_i} S(R_i)\Delta R_i} \qquad (13)$$

For simplicity, let's use the forms like $F_1(R_i) = F_1 p_1(R_i)$, then eq. (13) and (3) are re-arranged as follows:

$$\frac{F_1(R_i)}{F_1} = \frac{F_0(R_i) - W \dfrac{F_1(R_{i+1})}{F_1} \dfrac{S(R_{i+1})}{\Delta R_i}}{F_1 + WK_e(R_i) - W \dfrac{S(R_i)}{\Delta R_i} - \dfrac{3W}{R_i} S(R_i)} \qquad (33)$$

$$\sum_i \frac{F_1(R_i)}{F_1} = 1 \qquad (34)$$

$$F_1 + F_2 - F_0 = 3W \sum_i \frac{F_1(R_i)S(R_i)}{F_1 R_i} \qquad (35)$$

$$F_2(R_i) = W(R_i)K_e(R_i) \qquad (36)$$

식(33)을 원료흐름에 존재하는 모든 입자크기 간격에 확대 적용하면 입자크기의 간격수에 상당하는 식들로 구성된 연립방정식을 얻게 되는데, 이는 다음의 조건(식 34)이 만족될때까지 반복식으로 풀수 있다. 이후에는 총괄수지 (35), (36)으로부터 F2 및 그 입자분포를 구한다.

Gas phase balances

Taking the mixing and devolatilization times into account, we assume that the volatiles are released uniformly in the emulsion phase.

In the thesis of Kool, only two gas components are adopted in the balance. The rest gas components are calculated from stoichiometry.

Gas consumption due to the partial combustion of volatiles.

$$\Phi_{O2} = R_V Y_{O2}$$

Where R_V denotes volatiles released [mol/s] and Y_{O2} the oxygen required for the partial combustion of volatiles to CO [mol/mol].

$$\Phi_{CO} = R_{CO} + R_V Y_{CO}$$

Influence of char on:

O2 balance
The overall char combustion rate is found from

$$F_{ch,c} = -\int_o^\infty \frac{3\lambda(d) R_C(d)}{d} dd \qquad [kg/s] \qquad (3.5\text{-}14)$$

with

$$R_C(d) = \left(\frac{\partial d}{\partial t}\right)_C = -24\beta \frac{1}{\rho_{ch}} k_c(d) \overline{C}_{O_2,e} \qquad (3.5\text{-}7)$$

Based on reaction (3.2-3) the overall oxygen consumption [kmol/s] due to char combustion is given by:

$$\Psi_{O2} = \frac{1}{\Phi}\frac{F_{ch}}{12} = \frac{6}{\rho_{ch}}\int \frac{\lambda\ k_C}{\Phi d} dd \cdot \overline{C}_{O_2,e}$$

$$\Psi_{O_2} = \zeta_{O_2}\overline{C}_{O_2,e} \qquad (3.5\text{-}18)$$

where $$\zeta_{O_2} = \frac{6}{\rho_{ch}}\left[\int_0^{\infty} \frac{1}{\Phi(d)}\frac{\lambda(d)k_C(d)}{d} dd\right] \qquad (3.5\text{-}19)$$

CO_2 balance

Using

$$\zeta_{CO_2} = \frac{6}{\rho_{ch}}\left[\int_0^{\infty} \frac{(2\Phi(d)-2)}{\Phi(d)}\frac{\lambda(d)k_C(d)}{d} dd\right] \qquad (3.5\text{-}20)$$

the CO generation due to char combustion is given by

$$\Psi_{CO_2} = \zeta_{CO}\overline{C}_{O_2,e} \qquad (3.5\text{-}21)$$

In order to account for the influence on the mass balance over an incremental height interval we define

$$\Phi_{O_2}(z) = a(z)\Phi_{O_2} \qquad (3.5\text{-}22)$$

$$\Phi_{CO}(z) = a(z)\Phi_{CO} \qquad (3.5\text{-}23)$$

$$\Phi_{O_2}(z) = a(z)\Phi_{O_2}C_{O_2,e}(z) \qquad (3.5\text{-}24)$$

$$\Phi_{CO}(z) = a(z)\Phi_{CO}C_{O_2,e}(z) \qquad (3.5\text{-}25)$$

여기서 a(z)은 emulsion phase에서 height에 따른 fraction을 부여하는 함수로서 식(3.5-6)에 주어졌다

For bubble phase. O_2 balance

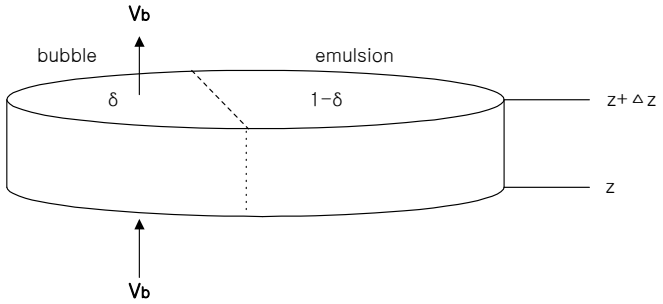

$$Acc = in - out + gen - concumption$$

$$\frac{\partial}{\partial t}\left[C_{O_2} \cdot A\Delta z\delta\right] = C_{O_2}V_b\big|_{\ z} - C_{O_2}V_b\big|_{\ z+\Delta z} - (A\Delta z\delta)k_{be}(C_{O_2} - C_{O_2}^*) - [A\Delta z\delta]k_{CO}C_{H_2O}^{0.5}C_{O_2}^{0.5}C_{CO} \quad \left[\frac{\text{mol}}{\text{s}}\right]$$

$C_{O_2}^*$: conc. at emulsion phase

divided by Δz & $\Delta z \to 0$

steady state

$$A\delta\frac{\partial C_{O_2}}{\partial t} = -\frac{\partial}{\partial z}\left(C_{O_2} \cdot V_b\right) - A\delta k_{be}(C_{O_2} - C_{O_2}^*) - A\delta\, k_{CO}C_{H_2O}^{0.5}C_{O_2}^{0.5}C_{CO}$$

$$V_b\frac{\partial C_{O_2}}{\partial z} + C_{O_2}\frac{\partial}{\partial z} = -A\delta k_{be}(C_{O_2} - C_{C_2}^*) - A\delta\, k_{CO}C_{H_2O}^{0.5}C_{O_2}^{0.5}C_{CO} \qquad (3.5\text{-}30)$$

CO balance

$$\frac{\partial}{\partial t}\left[C_{CO} \cdot A\Delta z\delta\right] = C_{CO}V_b\big|_{\ z} - C_{CO}V_b\big|_{\ z+\Delta z} - (A\Delta z\delta)k_{be}(C_{CO} - C_{CO}^*)$$
$$- [A\Delta z\delta]2k_{CO}C_{H_2O}^{0.5}C_{O_2}^{0.5}C_{CO}$$

as above,

$$\therefore\ V_b\frac{\partial C_{CO}}{\partial z} + C_{CO}\frac{\partial V_b}{\partial z} = -A\delta\, k_{be}(C_{CO} - C_{CO}^*) - 2A\delta\, k_{CO}C_{H_2O}^{0.5}C_{O_2}^{0.5}C_{CO}$$

$$\therefore\ \frac{dC_{CO}}{dz} = -\frac{1}{V_b}\left[2A\delta\, k_{CO}C_{H_2O}^{0.5}C_{O_2}^{0.5}C_{CO} + A\delta\, k_{CO}(C_{CO} - C_{CO}^*) + C_{CO}\frac{dV_b}{dz}\right] \quad (3.5\text{-}31)$$

For emulsion phase.

Plug flow condition (D_{AB}=0)

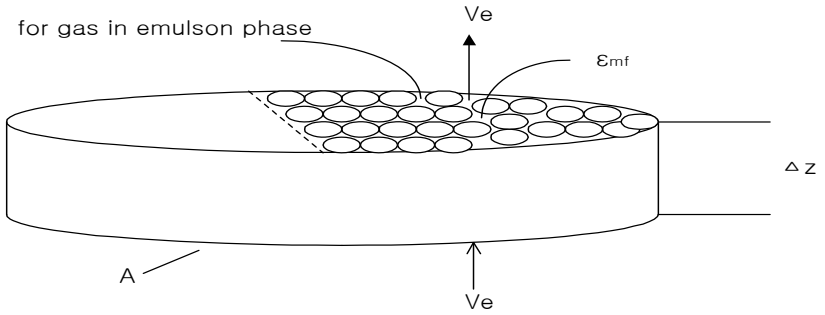

O_2 balance

$$Acc = in - out + gen$$

$$\frac{\partial}{\partial t}\left[C^*_{O_2}\cdot A\Delta z(1-\delta)\varepsilon_{mf}\right] = C^*_{O_2}V_e\big|_{\,z} - C^*_{O_2}V_e\big|_{\,z+\Delta z} - \Phi_{O_2} - \Psi_{O_2} + (A\Delta z\delta)k_{be}(C_{O_2} - C^*_{O_2})$$
$$- A\Delta z(1-\delta)\varepsilon_{mf}k_{CO}C^{*\,0.5}_{H_2O}C^{*\,0.5}_{O_2}C^*_{CO}$$

$\div \Delta z \;\; \& \;\; \Delta z \to 0$

$$\frac{d}{dt}\left[C^*_{CO_2}\cdot V_e\right] = -\Psi_{O_2} - \Phi_{O_2} - A(1-\delta)\varepsilon_{mf}k_{CO}C^{*\,0.5}_{H_2O}C^{*\,0.5}_{O_2}C^*_{CO} + A\delta k_{be}(C_{O_2} - C^*_{O_2})$$

$$\frac{dC^*_{O_2}}{dz} = -\frac{1}{V_e}\left[\Psi_{O_2} + \Phi_{O_2} + A(1-\delta)\varepsilon_{mf}k_{CO}C^{*\,0.5}_{H_2O}C^{*\,0.5}_{O_2}C^*_{CO} - A\delta k_{be}(C_{O_2} - C^*_{O_2}) + C^*_O\ \frac{dV_e}{dz}\right]$$

(3.5-36)

3.6 Heat transfer

Assuming a uniform bed temperature, the heat balance for the bed

$$\frac{d}{dt}\left(M_s c_s T_B\right) = E_1(t) - E_2(t) \qquad (3.6\text{-}1)$$

The energy generation rate is given by:

$$E_1 = \left(\Psi_{O2} - 0.5\Psi_{CO}\right)S_1 + 0.5\Psi_{CO}S_2 + R_V S_V + S_3 \int_0^{H_B} k_{CO} A_B(z) C_{H2O}^{0.5} \left[(1-\delta)\varepsilon_{mf} C_{O2,e}^{0.5} C_{CO,e} + \delta C_{O2,b}^{0.5} C_{CO,b}\right] dz$$ wit

h

S_1 = heat of reaction $\mathrm{C} + \mathrm{O_2} = \mathrm{CO_2}$, 3.97×10^5 kJ/kmol $\mathrm{O_2}$

S_2 = heat of reaction $2\mathrm{C} + \mathrm{O_2} = 2\mathrm{CO}$, 2.35×10^5 kJ/kmol $\mathrm{O_2}$

S_3 = heat of reaction $2\mathrm{CO} + \mathrm{O_2} = 2\mathrm{CO_2}$, 5.59×10^5 kJ/kmol $\mathrm{O_2}$

S_V = heat of volatiles combustion , kJ/kmol volatiles

R_V = volatiles released, kmol/s

The energy removing rate is given by:

$$E_2 = \alpha_t A_t (T_B - T_t) + F_g c_g (T_B - T_{in}) + F_{CO} c_{CO} (T_B - T_{in})$$

Heat transfer coefficient between bed and immersed cooling tubes,
By Glicksman & Decker (1980):

$$\alpha_t = (1-\bar{\delta})\frac{\lambda_g}{d_s}\left(9.3 + 0.042\,\mathrm{Re}\cdot\mathrm{Pr}\right) \qquad (3.6\text{-}5)$$

where λ_g = thermal conductivity of gas

3.7. Gas flow dynamics

Gas flow dynamics will be fast compared to char combustion and bed-heat up.
The combustor pressure is given by:

$$P_g = \rho_g R T_B = \frac{M_g}{V_g} R T_B \qquad (3.7\text{-}4)$$

Mass balance of gas inside the combustor volume:

$$\frac{dM_g}{dt} = F_{g,in} - F_{g,out} + (w_V + w_W) F_{CO,in} + F_{ch,C}$$

3.8. Numerical solution of the model.

우선은 steady-state conditions를 구한다음, 이후에 transient 거동을 구한다.

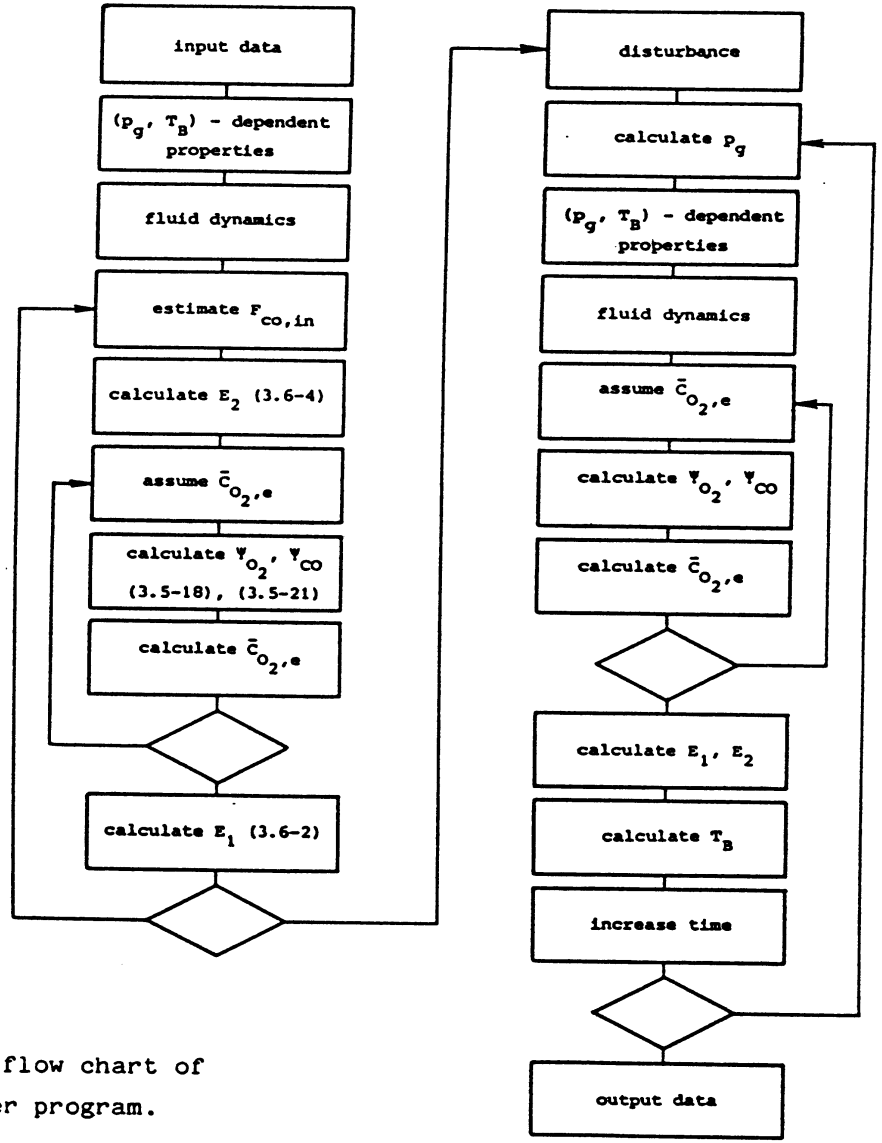

FIGURE 3-2.
Simplified flow chart of
the computer program.

3.9 Sensitivity Analysis

Analyse the impact of the main hypotheses and operating parameters on the model predictions.

Experimental facility referred for this simulation is shown in Fig. B-1

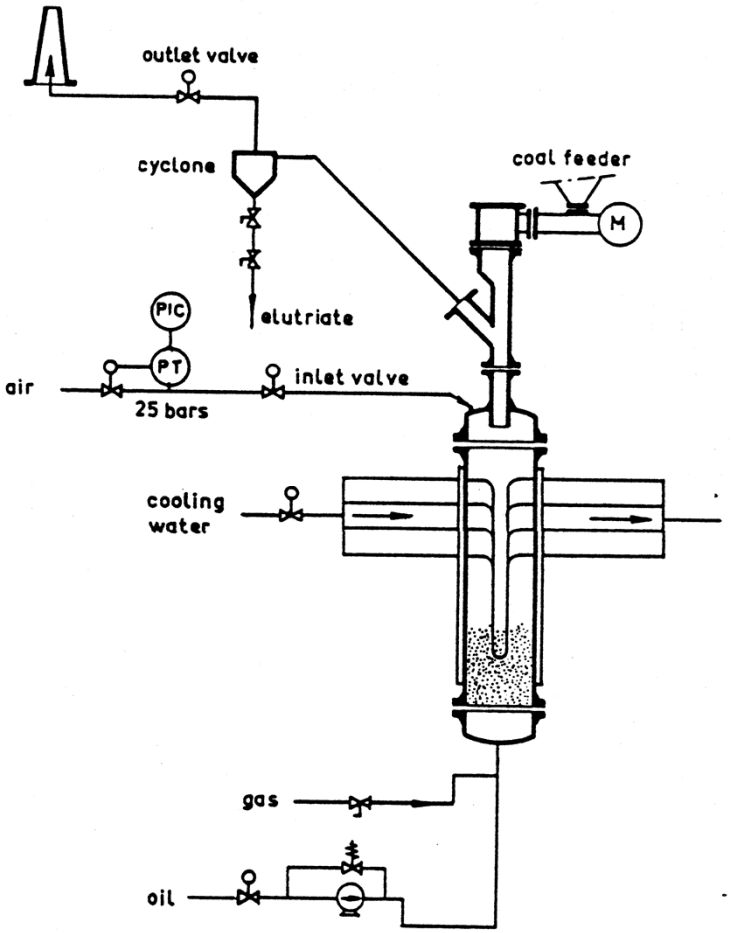

table 3.7.

proximate (%)		ultimate (%)	
moisture	1.7	carbon	87.1
volatiles	10.3	hydrogen	4.0
fixed carbon (dif.)	84.7	nitrogen	1.8
ash	3.3	sulphur	1.1
		oxygen (dif.)	2.7
		ash	3.3

TABLE 3-7.
Coal analysis: NBAG anthracite.

The values of the operating parameters taken as base case in this study are given in table 3-8.

pressure	0.5	MPa
bed temperature	1173.	K
fluidization velocity	1.05	m/s
flue gas oxygen concentration	5.	%

TABLE 3-8.
Base case operating parameters.

Important sub-processes = combustion

Kinetic relation of Smith (1970) for Anthracite
Kinetic relation of Field et al. (1967), which has widely been adapted

고압에서는 ks 형태의 영향이 줄어든다.
2 mm 입자의 경우 Field et al. 의 ks는 가압에 의한 연소속도의 증가가 Smith의 것보다 2 배의 증가를 보인다.

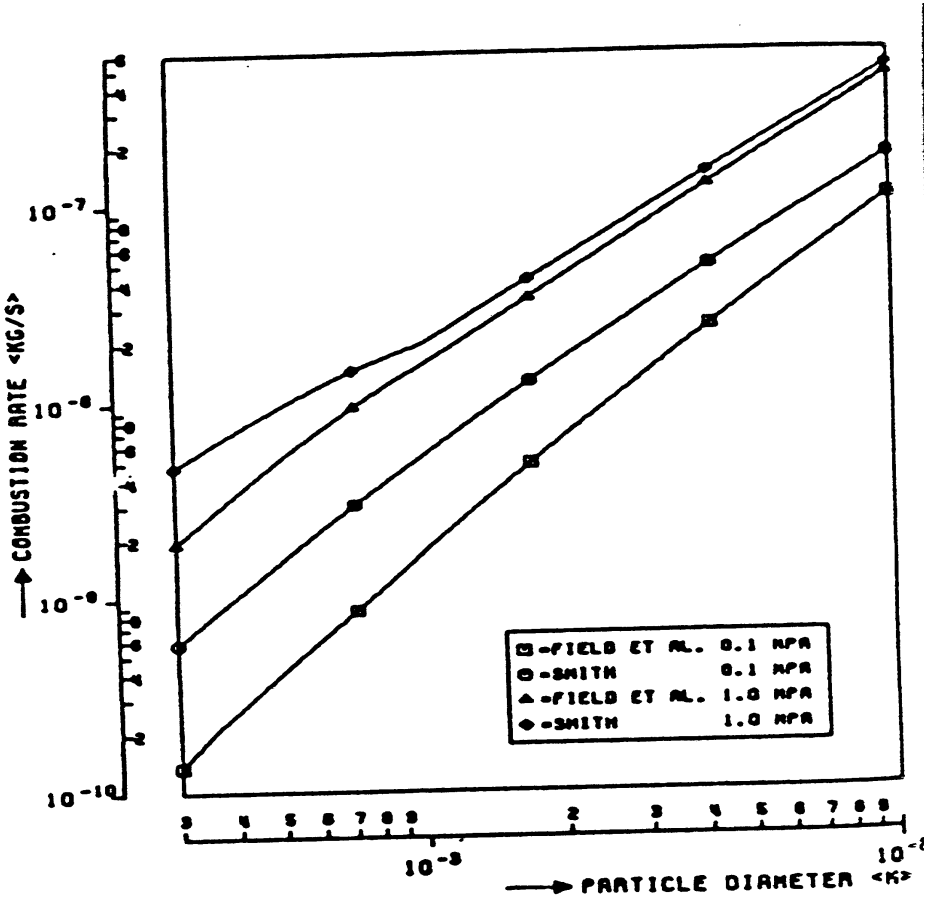

FIGURE 3-4.
Dependence of particle combustion rate on pressure.

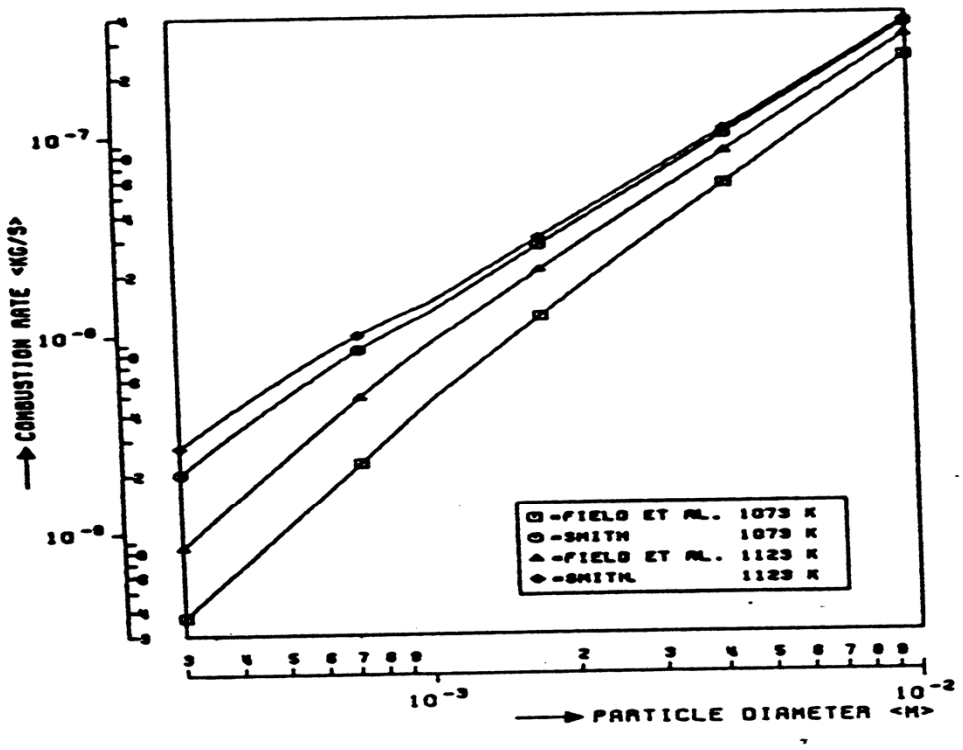

FIGURE 3-5.
Dependence of particle combustion rate on temperature.

높은 온도, 큰 입자에서는 ks 형태의 영향이 감소한다.
Field et al. 의 kinetic은 온도에 더 크게 좌우되고 있다.

Important sub-processes = fluidization/mixing

The parameter, γ, defining the flow distribution

$$\frac{V_b}{A_B} = \gamma(u - u_{mf})$$

The parameter, α, characterizing bubble growth:

$$d_b(z) = \alpha(u - u_{mf})\, z^{0.75}$$

상기 두 인자가 직접 관련된 것이 층의 팽창이다.
γ가 증가하면 기포들을 지름길로 사용하는 가스들이 적어지므로 층이 많이 팽창하게 된다. 그림으로부터 $0.5 < \gamma < 0.75$ 의 값을 구할수 있다. 그러나 α 값의 적절범위는 얻기 어렵다.

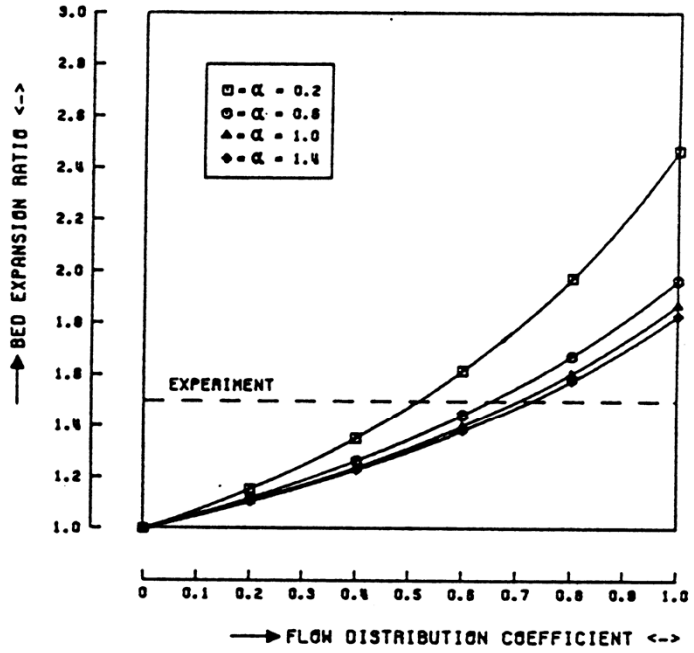

FIGURE 3-8.

Dependence of bed expansion on α and flow distribution coefficient γ.

원료탄이 층에 주입되어 초기 fragmentation을 겪은 후 층내에서의 촤의 입자크기분포

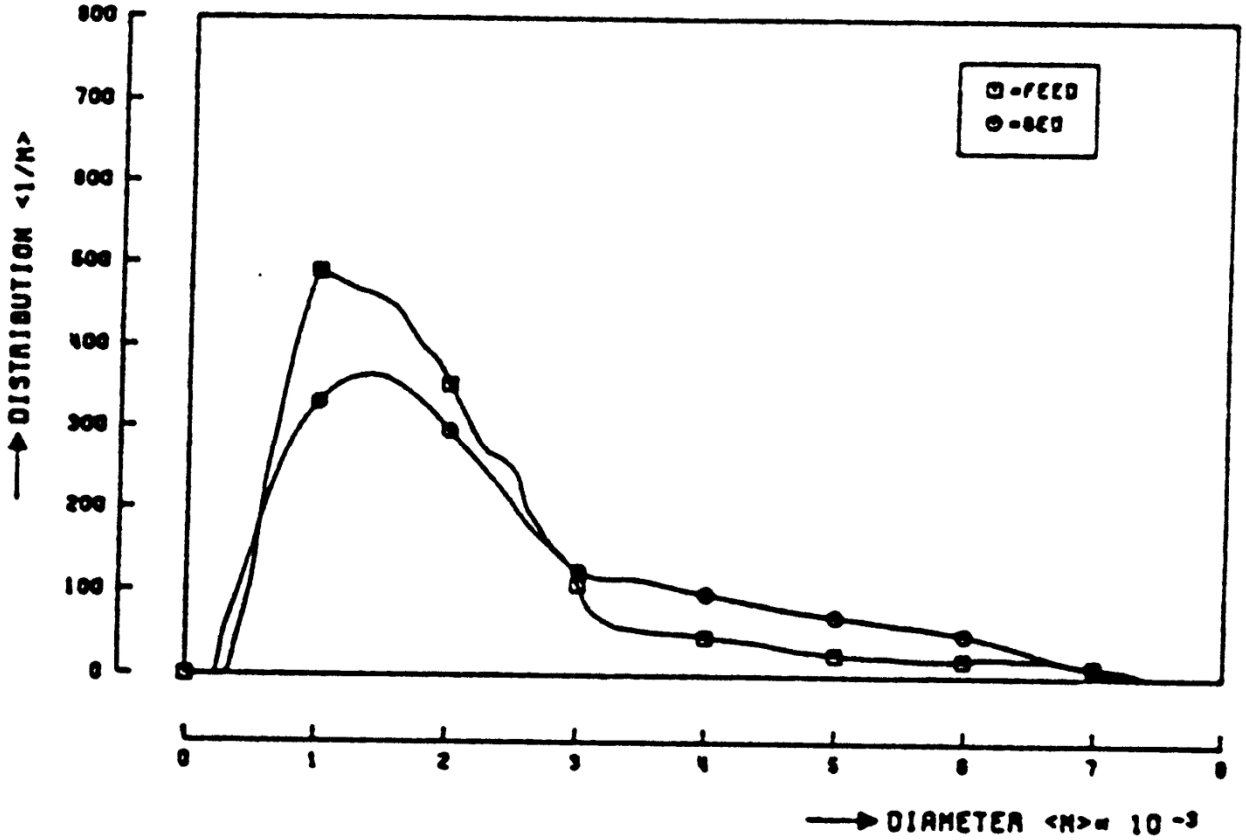

상이한 연소관련 가정에 따른 결과를 층내 탄소양을 주시하면 알 수 있다.
그림에서 Field et al. 의 kinetic을 사용한 경우는 반응성이 낮아서 층내 탄소량이 많이 남아 있음을 알 수 있다.

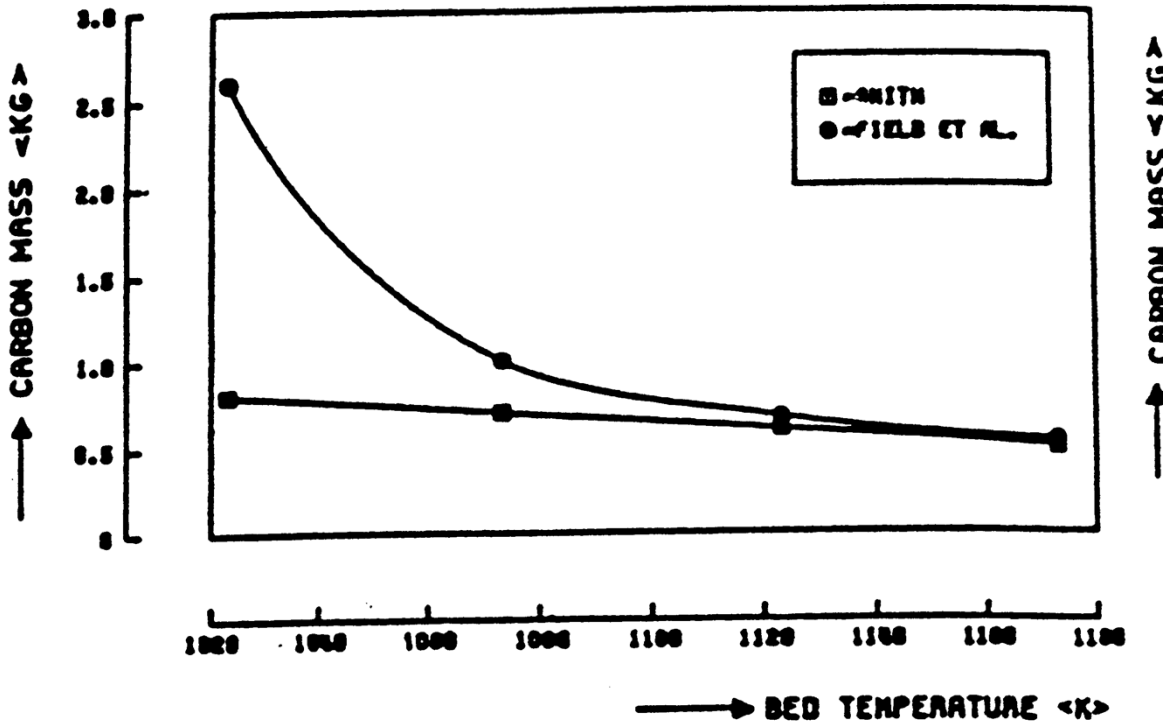

FIGURE 3-11.

Dependence of carbon mass

in the bed on temperature.

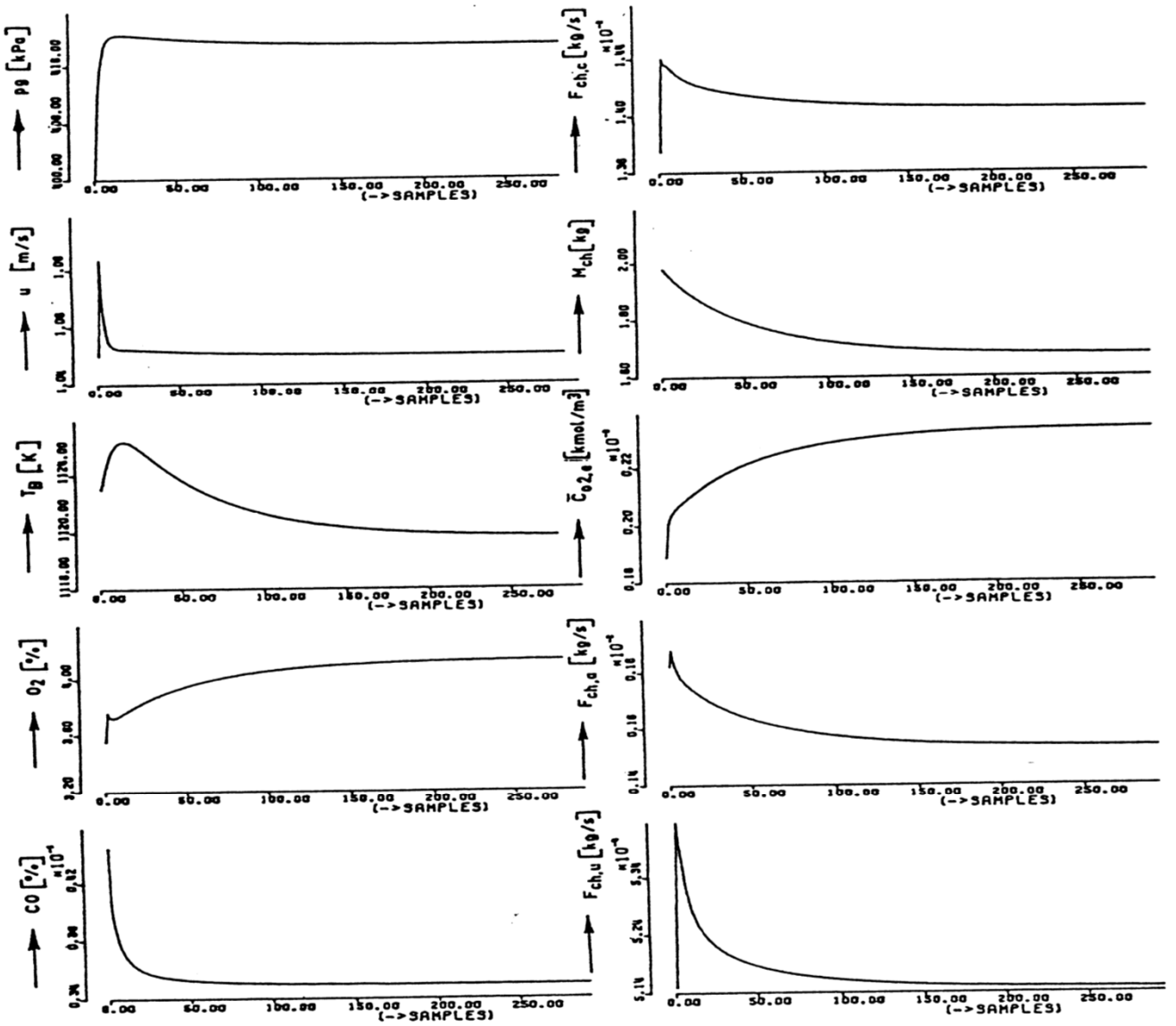

FIGURE 3-14.
Model responses to step in air flow (1 sample = 10 [s]).

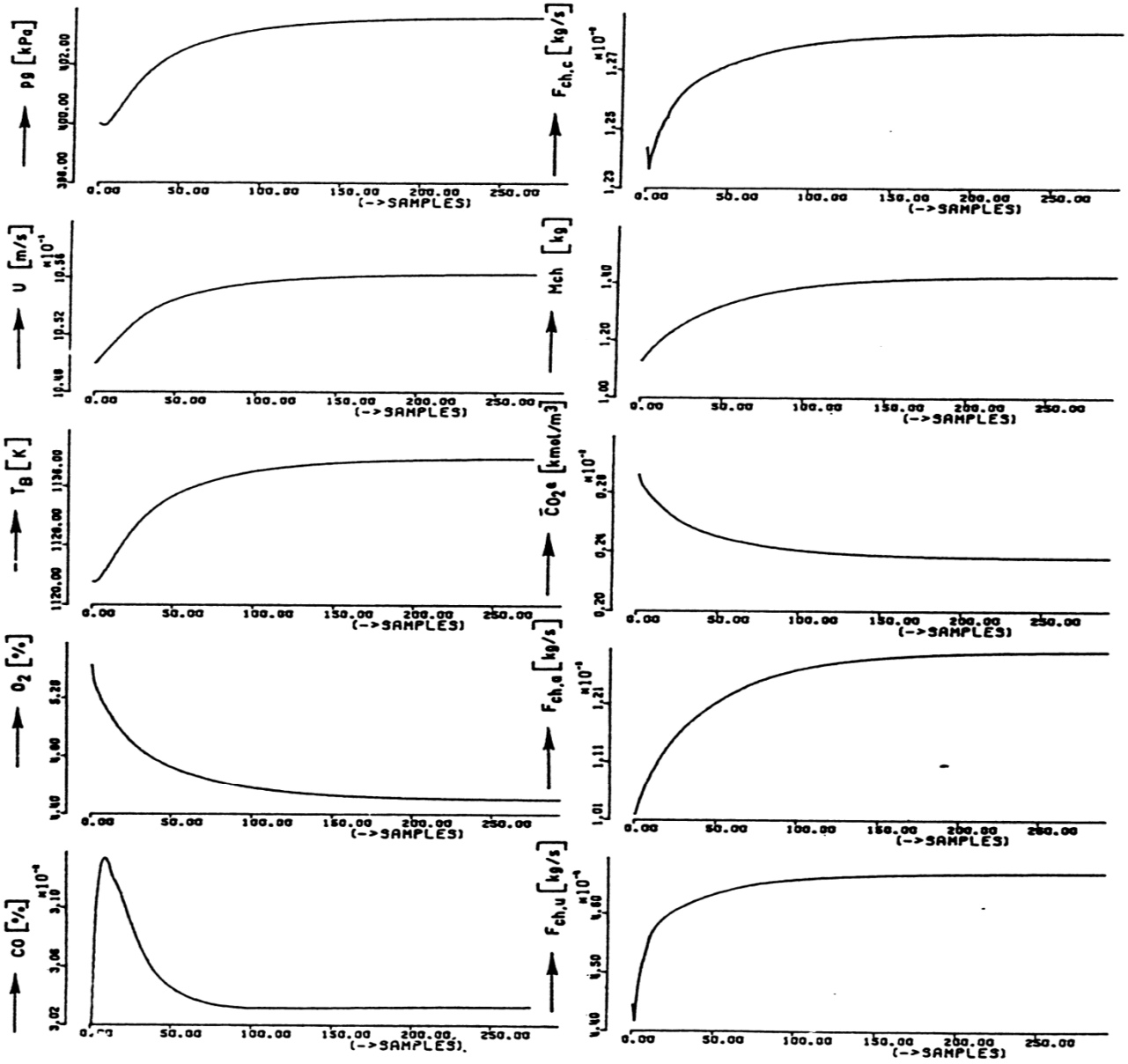

FIGURE 3-15.

Model responses to step in coal feed rate (1 sample = 10 [s]).

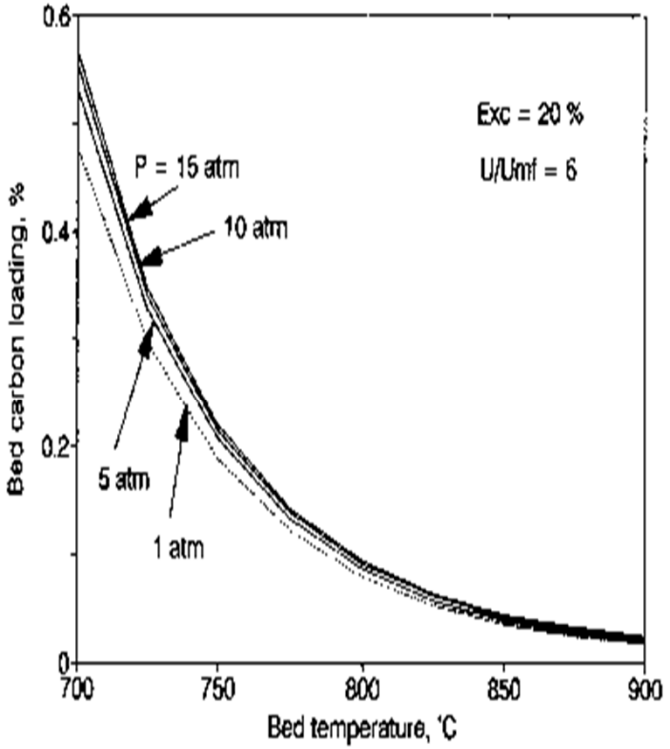

Fig. The change of the bed carbon loading with bed temperature

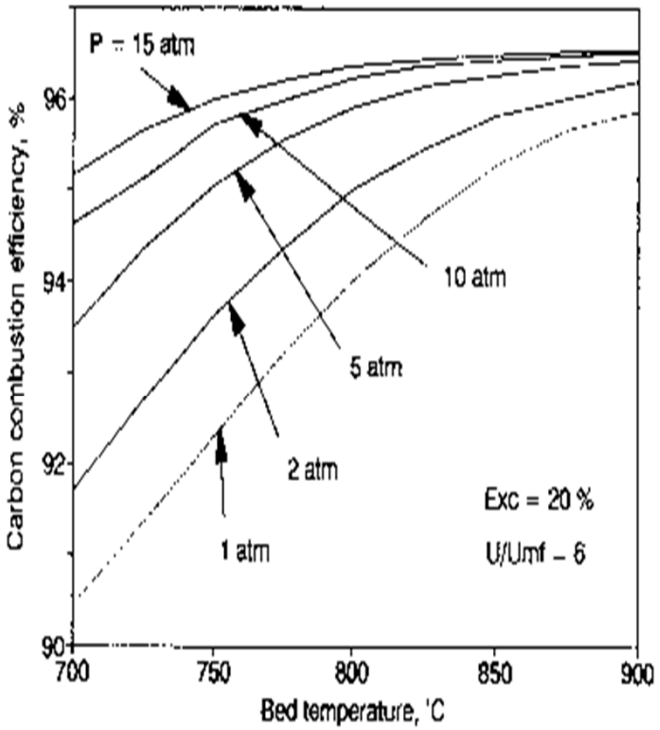

Fig. Effect of bed temp. on the carbon combustion efficiency

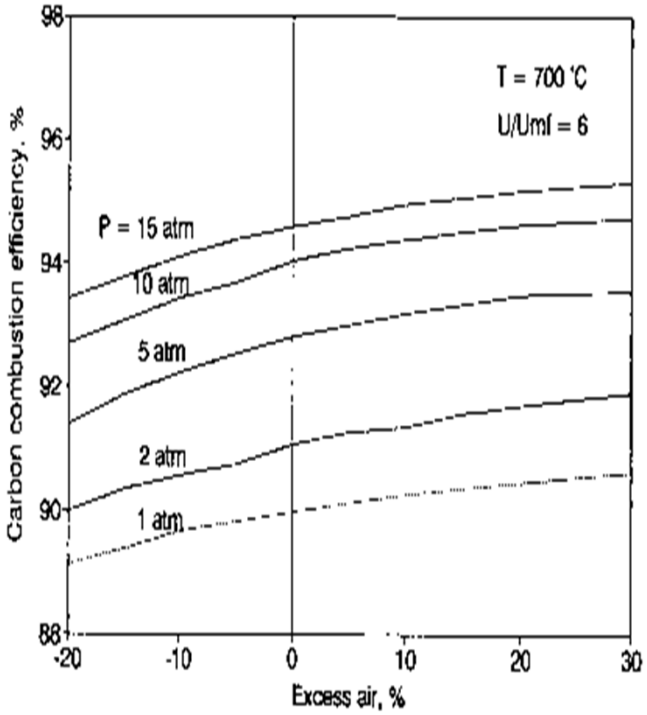

Fig. Effect of excess air on carbon combustion efficiency

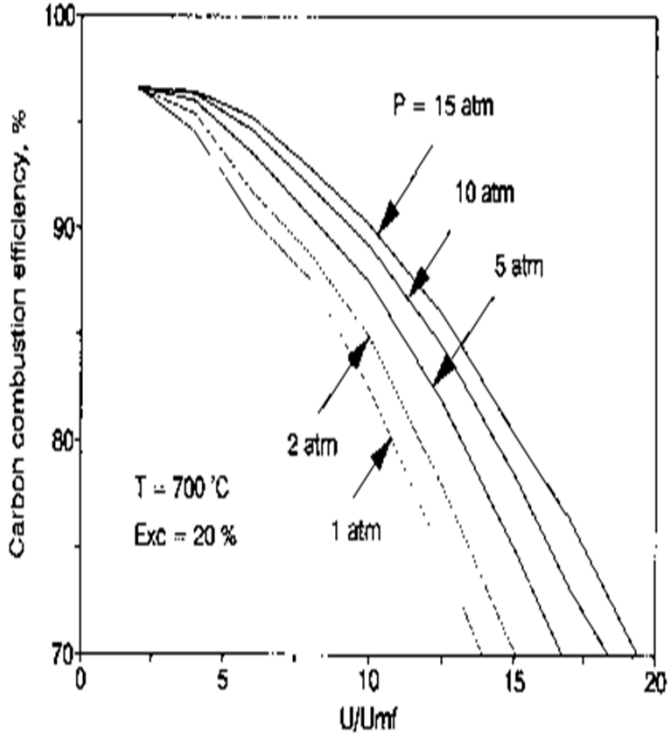

Fig. Effect of gas velocity on the carbon combustion efficiency

3. Conclustions

- 관련된 sub-process들에 대한 물리적인 정보가 부족한 것이 가장 큰 문제가 되고 있다.
-
연소는 비교적 낮은 온도에서 일어나고 있으며, fragmentation, attrition, elutriation에 의해 크게 좌우된다.
-
유동화거동 및 mixing은 주로 고체입자의 크기에 관련된다.
-